Regulation of a neuronal splice variant of Enabled homolog by N1-Src kinase in neurite outgrowth

Samuel Holliday

MSc by Research

University of York

Biology

May 2021

Abstract

The astounding complexity of the central nervous system arises from the precise guidance of axons to their synaptic targets. Aberrant axon guidance is implicated in neurodevelopmental disorders such as autism. At the distal end of the guiding axon, the growth cone receives signals that are transduced to the actin cytoskeleton. Principal players in these transduction pathways are non-receptor protein tyrosine kinases. One such kinase is N1-Src, a neural isoform of the ubiquitous c-Src, which is enriched in growth cone membranes and has altered substrate specificity from c-Src. The targets of N1-Src are poorly understood, but a preliminary substrate screen of N1-Src revealed an exciting potential candidate, a neural isoform of an actin regulator, N-Enah, with three putative tyrosine phosphorylation sites. Bioinformatic analysis demonstrated that N1-Src and N-Enah co-evolved in early vertebrate evolution. Interestingly, the *Drosophila* homologue of Enah, Ena, is tyrosine phosphorylated by Abl in a glutamine (Q)-rich domain that is not conserved in mammals. Ena tyrosine phosphorylation regulates protein-protein interactions necessary for the regulation of the actin cytoskeleton. In this project, it was hypothesised that the N-Enah insert and N1-Src function similarly to the Q-rich domain of Ena and Abl in neuronal differentiation. To investigate the function of N-Enah tyrosine phosphorylation, a phosphonull (6F) mutant of N-Enah was cloned into a Green Fluorescent (GFP)-expression plasmid and transfected into neuroblastoma cells with or without FLAG-tagged N1-Src. Compared to the wild type N-Enah, the 6F mutant could not be detected by immunoblotting with a phosphotyrosine antibody, was more stably associated with the cytoskeleton following subcellular fractionation, and inhibited cAMP-dependent neurite outgrowth. Taken together, these data support the idea that tyrosine phosphorylation of N-Enah regulates the interplay of protein-protein interactions necessary for actin polymerisation in neuronal differentiation. Further experiments are needed to identify the key players that are regulated by this conserved signalling mechanism.

List of contents

List of Figures and Tables

Acknowledgements

I am forever indebted to Gareth. Thank you ever so much for your excellent guidance, patience, and support throughout. Thank you to Gonz for sharing your wisdom in my TAP. And Liz, the light of my life, thanks to you I finally know who I am.

Author's declaration

I declare that this submission is entirely my own work, in my own words. All sources used in researching it are fully acknowledged, all quotations properly identified, and I am the sole author. This work has not previously been submitted for an award at this or any other university.

1 Introduction

1.1 Axon guidance in the developing brain

The billions of neurons and trillions of synapses that comprise neural circuits in the developed adult brain originate in the developing embryo. Although neurogenesis (the birth of neurons) persists throughout a lifetime, most of our brain cells are present by early postnatal stages (Mira and Morante, 2020). Healthy brain development requires precise guidance of axons to their synaptic targets in order for the vast number of connections to form (Stoeckli, 2018). A range of neurological disorders result from aberrant axon guidance processes.

How are neurons guided to their target cells? Neurons migrating through the pre-existing tissue of the developing brain are led by a structure at the distal tip of their axons. This structure, termed the growth cone, is like a hand in shape with finger-like membrane projections called filopodia and veil-like extensions called lamellipodia that are both rich in F-actin (filamentous actin) **(Figure 1)**. Ramon y Cajal discovered the growth cone in 1890 (Ramon Y Cajal, S., 1890). The cytoskeleton of the growth cone is highly dynamic in its ability to rapidly remodel F-actin, F-actin branching, F-actin treadmilling, and the links to and extensions of microtubules.

Roger Wolcott Sperry suggested that nerve fibres have a form of identification tag present on individual neurons (Sperry, 1963). In 1943, he rotated the eyeballs of developing newt embryos by 180 degrees. Sperry found that these newts moved their head in the opposite direction of a lure while control animals moved their heads predictably towards the lure (Sperry, 1943). This experiment led Sperry to assume a "definite specificity of central nervous system organisation… established in large part by growth processes" (Sperry, 1943). The fact that the nerve fibres were able to re-establish synapses at the tectum of the rotated eyes showed that they were not simply following predefined tracts but were instead

somehow being guided to their target cells. Sperry's resultant "chemoaffinity" hypothesis contrasted the more mechanical interpretation of Pierre-Ernest Weiss's "contact action" (Weiss, 1941). Work that followed Sperry's hypotheses revealed that fixed guidance cues such as intermediate targets act like sign posts to help the extending axons cross the relatively vast distances of the growing nervous system. Soluble guidance cues include molecular ligands that selectively stimulate growth responses of growth cones presenting their cognate receptors (Bashaw and Klein, 2010).

In attempts to determine the molecular nature of such guidance cues, Rita Levi-Montalcini and Viktor Hamburger showed that tumours implanted into chick embryos produced a diffusible "growth promoting agent" (Levi-Montalcini and Hamburger, 1953). This growth promoting agent selectively stimulated nerve fibres in the sympathetic and part of the somato-sensory system and was thus the first evidence of an axon guidance molecule. Later to be termed nerve growth factor (NGF), the discovery of this protein earned Levi-Montalcini the Nobel Prize in Physiology or Medicine along with Stanley Cohen in 1986. Levi-Montalcini "thought the active agent was a protein because it was heat-labile, non-dialyzable, and inactivated by a protease but not by DNase or RNase" (Cohen, 2008).

Grasshopper limb buds became a model system for investigating nerve development that led to the finding that glia cells formed a "system of signposts" (Bate, 1976). Staining of grasshopper embryos with antibodies revealed that subsets of axonal pathways were labelled with surface molecules, giving rise to the "labelled pathways" hypothesis (Goodman, 1984). Grasshopper limb buds were also used in the discovery of the semaphorin protein family of guidance molecules (Kolodkin et al., 1992).

Netrin-1 is one of the most studied guidance cues. Genetic experiments with *C. elegans* mutants for three genes, unc-5, unc-6, and unc-40, revealed them to be involved in axon guidance (Hedgecock et al., 1990). "Unc" is short for "uncoordinated" and was used to name many *C. elegans* genes involved in movement. Due to the axon guidance activity of two

novel proteins from embryonic chick brain, these proteins were named netrin-1 and netrin-2 as the root "netr" means "one who guides" in sanskrit (Serafini et al., 1994). Sequence homology of netrin-1 and netrin-2 cDNAs with unc-6 of *C. elegans* led to the establishment of this axon guidance protein family.

In addition to *C. elegans, Drosophila* proved to be a powerful genetic model for the discovery of axon guidance cues. A screen of over 13,000 *Drosophila* mutant embryos led to the discovery of two new genes: Commissureless (Comm) and Roundabout (Robo) (Seeger et al., 1993). Both Comm and Robo exhibited defects in midline crossing whereby comm mutant growth cones failed to cross the midline and robo mutants extended growth cones ectopically across the midline. Slit, an extracellular matrix protein, was identified as a ligand for Robo in further *Drosophila* genetic experiments (Brose et al., 1999). A technique that was used to test for this interaction between Robo and Slit was that, although single mutants of either gene were unlikely to produce a phenotype, double mutant genes, whose gene products directly interact, may produce a phenotype from the combined impairment.

1.2 Guidance molecules

Growth cones detect these guidance cues and transduce their signals into remodelling of the cytoskeleton to drive the morphological changes necessary to translocate the growing axon in the correct direction. Considering the complexity of connectivity found in large animals, there are a surprisingly small number of guidance molecules (Kolodkin and Pasterkamp, 2013), (Pasterkamp and Kolodkin, 2013), (Dent et al., 2011). Despite their diminutive number, the regulatory mechanisms that occur downstream of axon guidance receptors exemplifies the layers of complexity that arise from crosstalk between signalling pathways. Examples of axon guidance proteins and their receptors can be seen in Table 1. These molecules may be secreted, transmembrane, or GPI-linked (Glycosylphatidylinositol-linked) to the membrane.

Table 1 - Axon guidance proteins. Many proteins involved in axon guidance have been discovered. These molecules attract or repel growing axons and some have both functions. Guidance molecules may be secreted proteins, or may be transmembrane proteins, or may be linked via glycophosphatidylinositol (GPI-linked) to the external surface of the cell membrane. Guidance signals that ultimately lead to the rearrangement of the dynamic actin cytoskeleton are transduced from these molecules to their cognate receptors. The many downstream signalling targets exemplify dynamic nature and regulation required in the motile growth cone. Table adapted from (Kolodkin and Pasterkamp, 2013).

Guidance molecule	Location	Chemotrophic effect	Receptor	Coreceptor	Downstream Signalling Targets
EPHA	Transmembrane	Repulsion Attraction	EPHRINA EPHRINA	P75 RET	FYN -
EPHB	Transmembrane	Repulsion	EPHRINB	-	CDC42, DOCK180, GRB4, NCK2, PAK, RAC1
NETRIN	Secreted	Attraction	DCC	APP, HSPG, ROBO1	CDC42, DOCK180, **ENA/VASP**, ERK1/2, FAK, FYN, NCK1, NWASP, PAK, PI3K, PIP2, PKC, RAC1, RHOA, TRIO, TRP
		Repulsion	UNC5	DCC	FAK, SHP2, SRC
RGM	GPI-linked	Repulsion	NEOGENIN	UNC5	FAK, LARG, LMO4, MYOIIA, p120GAP, PKC, RAS, RHOA
PLEXINA	Transmembrane	Repulsion	SEMA1a	-	PEBBLE, RHO, p190RHOGAP
SEMA2	Secreted	Repulsion Attraction	PLEXINB PLEXINB	- -	RAC, RHO -
SEMA5	Transmembrane	Repulsion Attraction	PLEXINA1 -	CSPG HSPG	- -
SLIT	Secreted	Repulsion	ROBO	HSPG	CDC42, CROSSGAP, DOCK, RAC1, RHOA, SOS, SRGAP
SHH	Secreted	Repulsion	BOC	-	ILK, PKC,

					SMOOTHENED
		Attraction	BOC	-	FYN, SRC, SMOOTHENED
SFRP	Secreted	Attraction	Frizzled	-	Gα

Guidance molecule receptors are expressed on the growth cone membrane where the axon is navigated to its target cell (Stoeckli, 2018). Following interaction with their receptors, the information transduced from guidance molecules ultimately leads to morphological changes in the growth cone cytoskeleton (Kolodkin and Pasterkamp, 2013). The presence of coreceptors on the growth cone membrane may influence the chemoattractive effect. For example, binding of secreted Netrin-1 to DCC (Deleted in Colorectal Cancer) may lead to homodimerisation of DCC and a chemoattractive response or heterodimerisation of DCC with UNC5 which triggers repulsion (Boyer and Gupton, 2018). Secreted guidance molecules such as Netrin-1 form chemotactic gradients that mediate their effect over long distances while short-range haptotactic gradients are also present in the form of substrates that are bound to cells or the extracellular matrix (Boyer and Gupton, 2018).

To aid with the navigation over long distances, migrating growth cones are attracted towards intermediate targets, or choice points, but must switch to a repulsive response in order to move on (Stoeckli, 2018). Failure of a nerve to stop can result in nervous system defects such as a mutation in the Drosophila gene Enabled in which the Intersegmental nerve b fails to turn at contacts between muscles 14 and 28 in the developing embryo (Wills et al., 1999).

1.3 The growth cone is a hub of cytoskeletal regulation in axon guidance

The growth cone navigates its environment (Figure 1) at the distal tip that constantly probes its environment (Dent et al., 2011). The growth cone is like a hand in shape with finger-like membrane projections called filopodia and veil-like extensions called lamellipodia that are

both rich in F-actin (filamentous actin) (Figure 1) (Dent et al., 2011). Polymerisation of bundled actin exerts a pushing force on the membrane (Dent et al., 2011). Bundled filaments are stiff enough to form protrusive filopodia while non-bundled filaments are not (Lebrand et al., 2004). In a region of protruding growth cone, bundled actin polymerises to extend filopodia; a dense F-actin meshwork forms; and F-actin is severed to provide new barbed ends for monomer addition (Fig 1.1B). Bundled actin also provides the tracks that guide microtubules which in turn provide tracks for the transport of membranous vesicles needed for membrane extension (Fig 1.1C). The events that drive membrane protrusion are reversed in a retracting portion of the growth cone (Fig 1.1D).
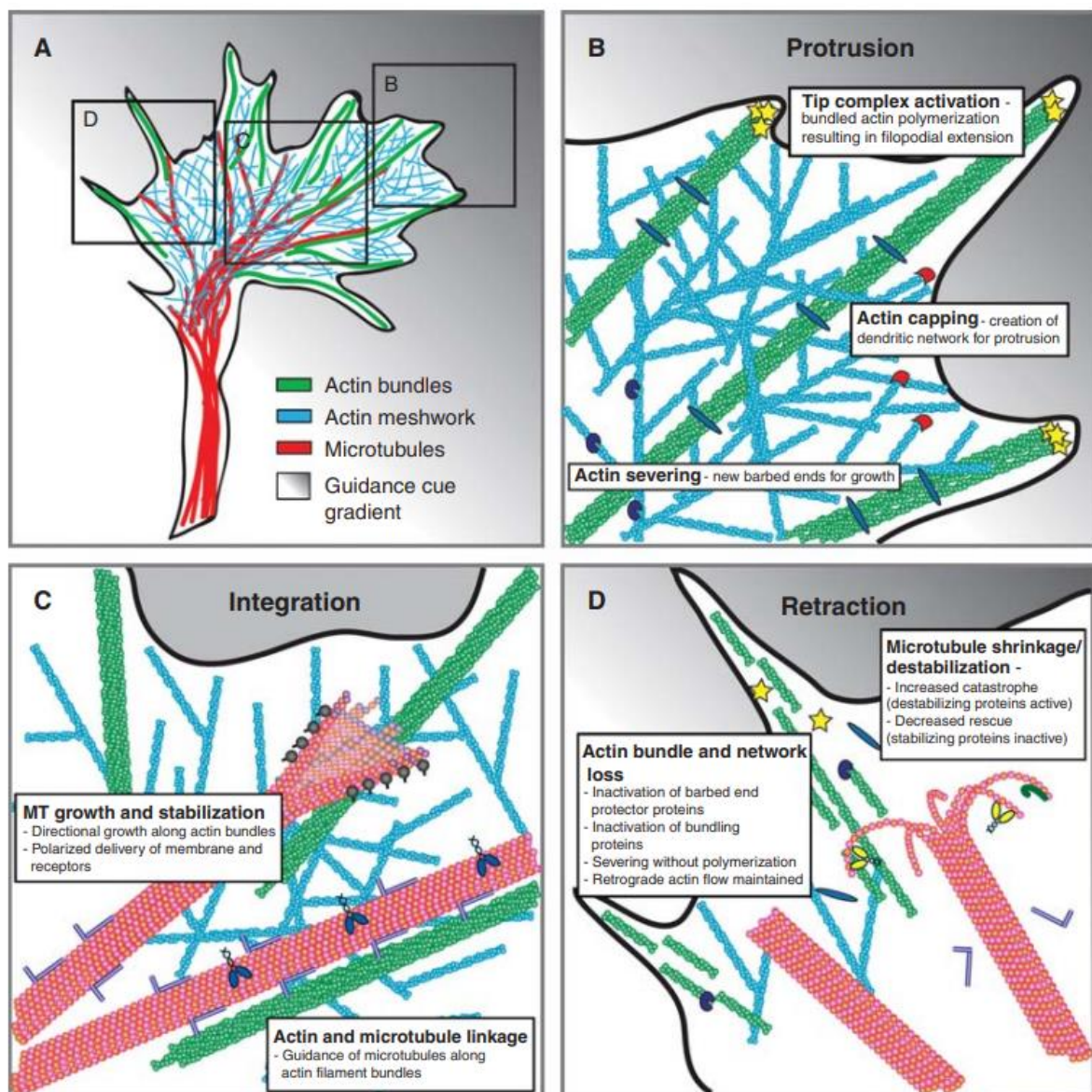
Figure 1. A model for the growth cone in axon guidance. An attractive guidance cue exists in a gradient with higher concentration towards the upper right. The growth cone extends towards and retracts away from the higher and lower concentrations of the guidance cue, respectively, turning towards the right. Actin bundles are green, actin meshwork is blue and microtubules are red (Figure taken from (Dent et al., 2011).

Cultured neurons are still able to extend their axons in the presence of agents that depolymerise F-actin but these axons do not respond to guidance cues (Dent et al., 2011). The dynamic F-actin network and its ability to form and depolymerise F-actin bundles and branches is primarily responsible for growth cone protrusion, motility, and the sensing of the environment (Dent et al., 2011). As the growing end of the actin filaments - the barbed ends - are at the distal tips near the membrane, addition of G-actin (globular actin) monomers contributes both to the pushing force on the membrane and the 'treadmilling' effect also known as retrograde actin flow (Dent et al., 2011).

Axon guidance is involved in neurodevelopmental disease. Autism Spectrum Disorders (ASD) and schizophrenia are examples of neurodevelopmental disorders that involve aberrant formation of neural circuits (Stoeckli, 2018). (Gilman et al., 2012) generated clusters of genes according to genetic phenotypes using an algorithm. These data were derived from whole-genome datasets associated with Schizophrenia. Further computational analysis of the resultant gene clusters used the over-representation of Gene Ontology (GO) terms to predict functions for these genes. "Axon guidance" and "Regulation of protein kinase activity" were amongst the most significant GO terms identified from the Schizophrenia gene clusters (p values were 1.54×10^{-5} and 1.87×10^{-5}, respectively).

Axon guidance is involved in neurodegenerative disease. The disintegration of neural circuits causes neurodegenerative diseases such as Alzheimer's and Parkinson's (Stoeckli, 2018). Antonell et al (2013) identified differentially expressed genes in sporadic Early Onset Alzheimer's Disease patients and patients of Familial Alzheimer's Disease caused by

PSEN1 mutations (FAD-PSEN1). Amongst the biological pathways identified were those related to axon guidance.

1.4 Signal transduction from guidance cues to actin remodelling

How are the signals from guidance cues integrated into the remodelling of the actin cytoskeleton? A myriad of actin associated proteins in hundreds of cell types contribute to the dynamic nature of the actin cytoskeleton in processes such as polymerisation, depolymerisation, barbed end capping, actin filament bundling, and contraction. One of these actin regulatory proteins is called Enabled.

The *Drosophila* gene enabled (Ena) was discovered in screens for genes that alleviate the lethal central nervous system phenotype (in which the rhabdomeres of the eye are misshapen leading to aberrant structural morphology of the ommatidial array) caused by loss of the non-receptor tyrosine kinase D-Abl (Gertler et al., 1990). As axons need to migrate large distances, choice points in the surrounding pre-existing tissue, termed intermediate targets, provide guidance cues. Growth cones switch responsiveness to guidance cues at intermediate targets from attractive to repulsive in order to move on, otherwise they would be stuck there (Stoeckli, 2018). Another *Drosophila* Ena mutation is an example of a failure in this switch mechanism and results in the intersegmental nerve b (ISNb) nerve failing to turn at contacts between muscles 14 and 28 in the developing embryo (Wills et al., 1999).

1.5 *Drosophila* enabled homologs in vertebrates

Mouse cDNA libraries were screened to find a mammalian homolog to *Drosophila* enabled which was termed Mena (mammalian ena) (Gertler et al., 1996). In the same study, Mena was then used to screen a mouse brain cDNA library, which identified three alternative splice variants - all contained a large insert coding for 246 amino acids and some contained one of

two additional sequences that code for four or 19 amino acids. Two more proteins were identified as having related sequences to Mena through further database searches. These were VASP (vasodilator-stimulated phosphoprotein) and a novel protein isolated by screening a murine cDNA library with an expressed sequence tag. The new protein was termed EVL (Ena/VASP-Like). Together, Mena, VASP, and EVL comprise a family of related proteins in vertebrates (Kwiatkowski et al., 2003). Vertebrates possess three paralogs to *Drosophila* Ena: Mena, EVL, and VASP (Figure 2). Mena is henceforth referred to as Enah for 'Enabled homolog' in this study.
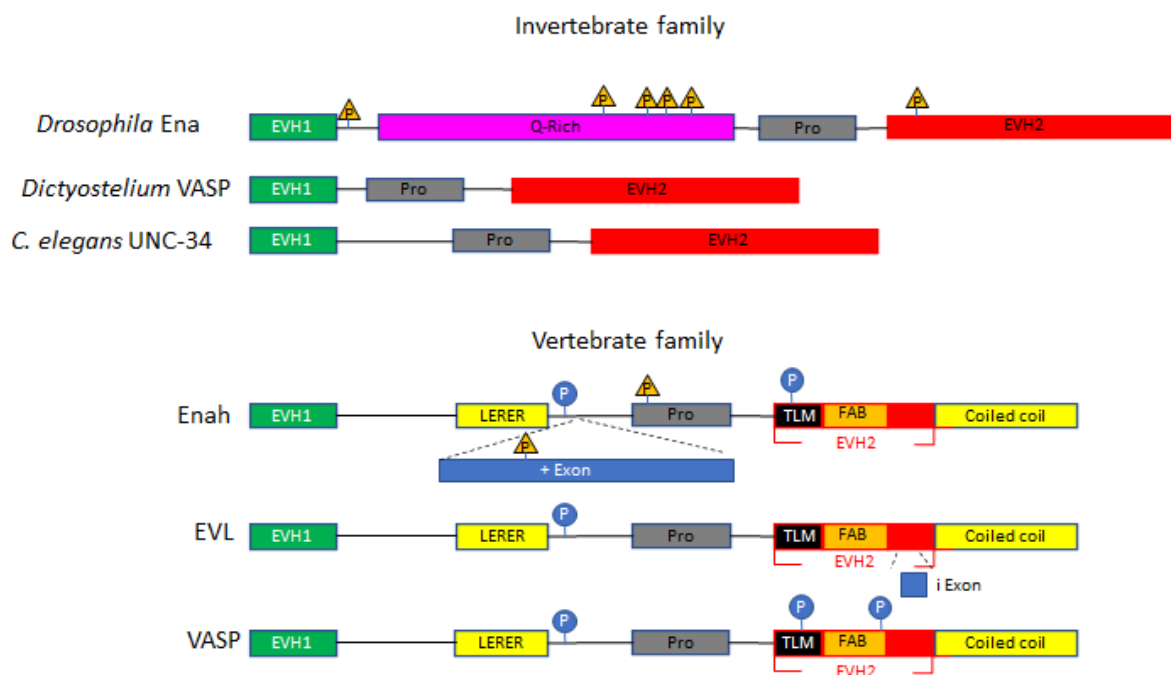
Figure 2. Domain structures of related sequences to *Drosophila* Ena. Invertebrates have one homolog (top) while vertebrates possess three paralogs (bottom). The EVH1 (Ena/VASP Homology 1) domain is at the N-terminus. *Drosophila* Ena has a glutamine-rich region. All proteins have a proline-rich region near the core. The EVH2 (Ena/VASP Homology 2) domain is at the C-terminus in all sequences. A conserved PKA (protein Kinase A) phosphorylation site is present in the vertebrate family. Enah (Mena) and EVL have a neuron-specific exon as indicated. Enah also has a tandem repeat region with consensus sequence LERER. TLM, (Thymosin-Like Motif) binds to G-actin monomers. FAB, F-actin-binding region. Phosphoserine/ phosphothreonine sites indicated by a P in a blue circle and phosphotyrosine residues are labelled with a P in an orange triangle although their precise positions are not all known. Adapted from a review by (Kwiatkowski et al., 2003).

1.6 The role of Src kinases in neuronal development

The regulatory mechanisms underlying crosstalk between different guidance cues and their receptors is more important than the discovery of new guidance molecules (Stoeckli, 2018). Phosphorylation of FAK (Focal Adhesion Kinase) is induced by netrin-1 and FAK is required for the netrin-1-dependent axon attraction and axon outgrowth-promoting activities (Liu et al., 2004).

Expression patterns and substrates identified for non-receptor protein tyrosine kinases (PTKs) indicate roles in neuronal development. c-Src is preferentially expressed in the nervous system and alternatively spliced in vertebrates. Neural cell adhesion proteins of the immunoglobulin superfamily, such as N-CAM and L1, bind to growth cone membrane proteins, reducing c-Src-induced phosphorylation of tubulin. Therefore, signals are transduced from cell adhesion molecules to the growth cone cytoskeleton via non-receptor PTKs (Maness, 1992).

The PC12 cell line is derived from tumour tissue of the rat adrenal gland and has been used as a model for neuronal differentiation in response to NGF stimulation. NGF was found to stimulate a receptor tyrosine kinase, TrkA, in PC12 cells, stimulating neurite outgrowth (Sierra-Fonseca et al., 2014). NGF-independent differentiation of PC12 cells has been achieved through infecting the cells with a temperature-sensitive form of pp60[v-src], a version of c-Src coded for by the Rous Sarcoma virus (Maness, 1992). In addition to enhancing neurite extension, tyrosine phosphorylation of α-Tubulin was also observed following infection with pp60[v-src] (Cox and Maness, 1991). Therefore, tyrosine phosphorylation by non-receptor PTKs play a role in neurite extension and axon guidance.

1.7 C-Src and its neuronal splice variants

Src non-receptor tyrosine kinase was discovered in a virus affecting chickens called Rous

Sarcoma Virus. This viral protein, pp60[v-src], was found to be an oncogenic version of the

cellular counterpart, C-Src (Stehelin et al., 1976), and a member of a group of 11 related

kinases, the Src family kinases (SFKs). The name Src comes from sarcoma. A neuron-

specific Src isoform was found in a mouse cDNA library (Martinez et al., 1987). C-Src has

two neuron-specific isoforms, N1-Src and N2-Src, with six and 17 residues inserted into the

SH3 (Src Homology 3) domain between exons 3 and 4, respectively (Figure 3) (West et al.

2019). N1-Src has been implicated in neuronal development (Lewis et al., 2017).
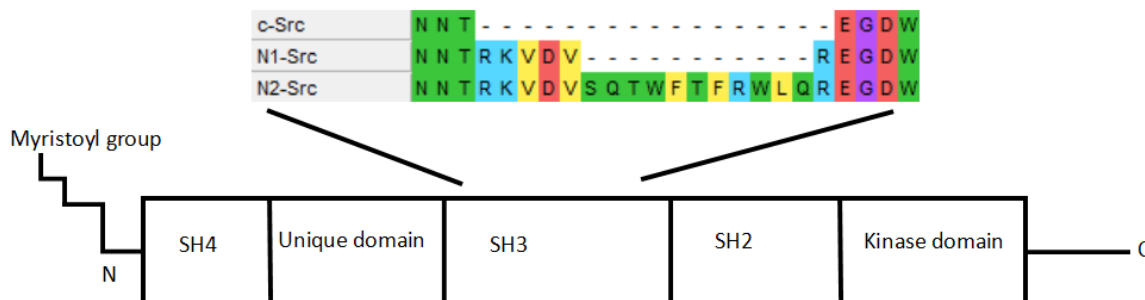
Figure 3. Domain structure of C-Src. The microexon insertions of N1-Src and N2-Src are shown.

N1-Src has been implicated in neurite outgrowth as ablation of N1-Src by shRNA knockdown

or a peptide inhibitor, PDN1, was shown to inhibit L1-CAM dependent neurite elongation in

cerebellar granule neurons (Keenan et al., 2017). Preliminary work by the Evans lab

involved screening for SH3 ligands and substrates of C-Src and N1-Src, using SH3-pulldown

assays or *in vitro* kinase assays followed by mass spectrometry (West et al. 2019). Among

the ligands identified were a cluster of cytoskeletal regulators. Enah is one of these actin

regulators and has a neural-enriched isoform, N-Enah, which has a large (246 amino acid)

insert (Gertler et al., 1996). Although identified in 1996 by Gertler et al, this neuron-specific

isoform of Enah remains largely uncharacterised. West et. al. observed preferential binding

of N1-Src (but not C-Src) to N-Enah over Enah, thus hinting at a potential role for N-Enah in N1-Src-mediated axon guidance, especially given the presence of N1-Src in growth cone membranes (Maness et al., 1988).

1.8 The phosphoregulation of Ena/VASP proteins

Phosphorylation of Ena/VASP proteins regulates interactions with other proteins necessary for functions including actin polymerisation. It is the regulation of such protein-protein interactions that allows the dynamic actin cytoskeleton to respond rapidly and precisely to signals transduced from external guidance cues. There are three phosphorylation sites in Ena/VASP proteins that are phosphorylated by PKA and PKG Serine/Threonine kinases (Krause et al., 2003) (**Figure 2**). VASP is phosphorylated by PKA and PKG at three sites (Butt et al., 1994) (**Figure 2**). The first two of these sites are also conserved in Enah (Gertler et al., 1996) while EVL possesses only the first site (Lambrechts et al., 2000) (**Figure 2**). Abl tyrosine kinase phosphorylates Ena (Comer et al., 1998) and possibly Enah (Tani et al., 2003) and interacts with VASP (Howe et al., 2002).

Drosophila Ena is tyrosine phosphorylated by *Drosophila* and Human Abl (Gertler et al., 1995). As previously stated, it was the genetic interaction between Ena and D-abl that led to the discovery of Ena. This D-Abl/Abl-dependent tyrosine phosphorylation of Ena has been suggested to negatively regulate Ena during the development of the nervous system (Gertler et al., 1995). As tyrosine phosphorylation of Ena is merely reduced in Abl mutant flies, and the SH3 domains of Src and Abl bind to Ena, this hints that other kinases likely tyrosine phosphorylate Ena (Krause et al., 2003). Two isoforms of Ena have been identified whereby the 80 kDa isoform is phosphorylated more on serine than tyrosine and the 100 kDa isoform is predominantly tyrosine phosphorylated (Gertler et al., 1995). However, Ena lacks the amino-terminal PKA site shared across all vertebrate Ena/VASP proteins (Gertler et al., 1996) so this phosphorylation site likely evolved in early vertebrates.

Two of the three aforementioned vertebrate PKA/PKG phosphorylation sites are present in Enah that flank the proline-rich region (PRR) (Gertler et al., 1996) (**Figure 2**). Netrin-1-induced filopodia require Ena/VASP proteins in which Enah is phosphorylated by PKA at S236, the conserved site in vertebrates (Lebrand et al., 2004). Enah, when overexpressed in cells with c-Abl and Abi-1, is tyrosine phosphorylated at Y-296 by c-Abl (Tani et al., 2003). However it remains to be demonstrated what is regulated by this and whether endogenous levels of Enah, Abi-1, and c-Abl cause phosphorylation at Y296 of Enah. Y296 is inside the PRR so this phosphorylation may disrupt interactions with the PRR such as SH3 domains of profilin.

Phosphorylation of VASP and Enah at the conserved vertebrate site (S135 in VASP) by PKA correlates with detachment of fibroblasts (Howe et al., 2002). Furthermore, both VASP and Enah are dephosphorylated at this site following binding to extracellular matrix proteins (Howe et al., 2002). This adhesion-dependent phosphorylation of VASP by PKA in turn regulates the interaction of c-Abl with VASP as c-Abl was only immunoprecipitated with dephospho VASP and not phospho VASP (Howe et al., 2002). The phosphorylation state of VASP did not affect its localisation to focal adhesions, its binding to focal adhesion proteins zyxin and vinculin, or binding to profillin (Harbeck et al., 2000). Following increasing incubation times of VASP with PKA, VASP co-sedimented less with prepolymerised F-actin (Harbeck et al., 2000). EVL binds preferentially to profilin-IIa, the major isoform of profilin in the brain, and to N-Src, Lyn, and c-Abl SH3 domains in vitro (Lambrechts et al., 2000). The binding of N-Src and c-Abl to EVL is abrogated by phosphorylation of EVL by PKA (Lambrechts et al., 2000).

Taken together, Ena/VASP proteins are phosphorylated by serine/threonine and tyrosine kinases. PKA phosphorylation appears to disrupt binding such as c-Abl and N-Src to EVL (Lambrechts et al., 2000); VASP with F-actin (Harbeck et al., 2000); and VASP and Enah

interactions with ECM proteins (Howe et al., 2002). Does the requirement for Enah to be phosphorylated at S236 for the netrin-1-induced filopodia extension (Lebrand et al., 2004) contradict the observations that dephosphorylated VASP is more effective at bundling and binding to F-actin? Ena/VASP proteins have been shown to negatively regulate fibroblast motility (Bear et al., 2000). This was later suggested to be due to the long actin filaments with reduced branching density, caused by overexpressed Ena/VASP, being less able to overcome the membrane tension following protrusion, leading to ruffles (Bear et al., 2002).

Tyrosine phosphorylation of Ena/VASP proteins is poorly understood. Ena is phosphorylated at multiple tyrosine residues in the PRR (Comer et al., 1998) and Enah phosphorylation at Y296 has been observed but not at endogenous levels of Enah (Tani et al., 2003).

1.9 Hypothesis and aims

In Laura West's PhD thesis (2019), N1-Src was found to preferentially bind N-Enah over Enah while C-Src does not have a preference for either isoform of Enah (West et al., 2019). As both the kinase (N1-Src) and the actin regulator (N-Enah) are neural isoforms that are enriched in neurons, this finding hinted at possible regulation of the actin cytoskeleton during axon guidance.

The large neural insert in the neuronal isoform of Enah, N-Enah, contains many proline residues and six tyrosine residues. The size of the PRR has been reduced from invertebrates to vertebrates. Abl-mediated phosphorylation of the six tyrosine residues in Ena inhibited the binding of SH3 domains (Comer et al., 1998), suggesting the balance of phosphorylation states of Ena dictates which proline-rich binding proteins associate with Ena to fine tune actin network dynamics. PKA phosphorylation of Ena/VASP proteins is possibly upstream of the tyrosine phosphorylation as phosphorylation of VASP by PKA blocks the binding of Abl to VASP (Howe et al., 2002).

It was hypothesised that the six tyrosines of the large N-Enah neural insert, that are potentially phosphorylated by N1-Src, recapitulate the six tyrosines found in Ena, and that phosphorylation of these tyrosines regulates the binding of other proteins.

In order to test this hypothesis, I will aim to develop an assay for neurite outgrowth in culture, in which the expression and activities of N1-Src and N-Enah can be manipulated. To further probe the role of N-Enah tyrosine phosphorylation, a construct will be designed that incorporates a phosphonull form of N-Enah with all six tyrosine residues of the neural exon mutated to phenylalanine (**Figure 6A**). The use of cAMP to stimulate PKA activation will also aid in the investigation of the phosphoregulation of N-Enah. This phosphonull mutant approach has been used to show that Ena is tyrosine phosphorylated by Abl and the mutation of six tyrosine residues in Ena to phenylalanine vastly reduced the detectable phosphotyrosine (Comer et al., 1998). Mammalian expression plasmids encoding N1-Src tagged with FLAG (Keenan et al., 2017) or mCherry are available.

2 Methods

Phylogenetic analysis

The amino acid sequences of N1-Src and N-Enah were taken from the ensembl (ensembl.org) and KEGG (genome.jp/kegg/genome/) genome browsers. These sequences were then aligned using Clustal Omega (ebi.ac.uk/Tools/msa/clustalo/). The tree data from Clustal Omega was then uploaded on iTOL (Interactive Tree Of Life, itol.embl.de/) for visualisation as unrooted phylogenetic trees.

Production of constructs

The N-Enah-WT plasmid was obtained from Dr Laura West and comprised a pEGFP-C1 backbone produced by Clontech and purchased from General Biosystems (Durham, North Carolina, USA). The gene insert codes for the 803 aa thought to be the neural isoform of Enah, N-Enah, of Rattus norvegicus fused to EGFP at the N-terminus, and flanked by BglII and BamHI restriction sites.

The N-Enah-6F plasmid was purchased from General Biosystems (Durham, North Carolina, USA). It has the same sequence as N-Enah-WT plasmid but has six tyrosine codons mutated to phenylalanine codons, in each case TAC → TTC: 809A→T, 830A→T, 869A→T, 914A→T, 1031A→T, 1298A→T.

Cell culture

The B104 neuroblastoma cell line from ECACC was grown in DMEM (High Glucose, + L-Glutamine, - HEPES, + Pyruvate) from ThermoFisher (41966-029), with 10% FCS and 1% penicillin/streptomycin, in an incubator at 37°C and 5% CO_2.

Transfections

For 24-well plates, 2.5 x10^4 cells were plated in 1 mL DMEM (High Glucose, + L-Glutamine, - HEPES, + Pyruvate) (41966-029 from ThermoFisher scientific, Paisley, Scotland), with 10% FCS and 1% penicillin/streptomycin onto 13 mm glass coverslips. The following day, the media in each well was replaced with 0.5 mL DMEM, 10% FCS, 1% penicillin/streptomycin 1 h prior to transfection. PolyJet transfection reagent, 1.5 µL per well, from SignaGen, was diluted in 25 µL DMEM per well, pipetted up and down four times, and then immediately added to 0.5 µg of each DNA construct per well also diluted in 25 µL DMEM per well. Following 10 min of incubation at room temperature, the PolyJet-DNA complexes were dispensed dropwise onto each well. The media was changed the next day with 1 mL of either DMEM 10% FCS 1% penicillin/streptomycin or DMEM 2% FCS penicillin/streptomycin + 1 mM db-cAMP.

For 6-well plates, 1x10^5 cells in 2 mL DMEM 10% FCS 1% penicillin/streptomycin were plated in each well. The following day, the media in each well was replaced with 1 mL DMEM, 10% FCS, 1% penicillin/streptomycin 1 h prior to transfection. 3 µL per well of the PolyJet transfection reagent, from SignaGen, was diluted in 50 µL DMEM per well, pipetted up and down four times, and then immediately added to 1 µg of each DNA construct per well, or 0.5 µg of each construct in co-transfections, also diluted in 50 µL DMEM per well. Following 10 min of incubation at room temperature, the PolyJet-DNA complexes were dispensed dropwise onto each well. The media was changed the next day with 2 mL of either DMEM 10% FCS 1% penicillin/streptomycin or DMEM 2% FCS 1% penicillin/streptomycin.

Cell morphology experiment

B104 cells were transfected with either GFP, N-Enah-WT, or N-Enah-6F as above for 24-well plates such that there were four wells per construct. In each set of four wells, two wells had the media replaced with DMEM 10% FCS 1% penicillin/streptomycin and the other two received DMEM 2% FCS penicillin/streptomycin + 1 mM db-cAMP. Four days later, the cells were washed three times with 0.5 mL PBS, fixed in 4% paraformaldehyde + sucrose for 20 minutes, washed three more times with 0.5 mL PBS, washed a final time in 0.5 mL dH$_2$0 and air dried. The coverslips were then mounted on glass slides with Mowiol-DAPI and were blinded by covering up the text with tape and shuffling them before numbering them. Images were taken with the Nikon TE200 microscope using the Nikon DXM 1200 digital camera. Images were analysed with the ImageJ software with the NeuronJ plugin. Neurites were counted as protrusions from the cell body that were at least 10 μm long and approximately 2 μm thick. The number of puncta were counted using the Spot counter plugin for ImageJ/FIJI: using a Box Size of 1 and a Noise Tolerance of 60.

Single pixels were ignored if they were outside the cell. Single pixels inside the cell were included because they couldn't be distinguished from noise and would be controlled for in the GFP control cells.

The size of puncta were measured using the SQUASSH plugin for ImageJ/FIJI.

Western Blot

Cells in 6-well plates were lysed with 150 μL Laemmli buffer while being scraped with a pipette tip. The cell lysates were boiled using a heat block before 20 μL of each sample was deposited in each lane of a SDS-PAGE gel (10% polyacrylamide). Transfer from gel to PVDF membrane was carried out at 20 V overnight (16 h). Membranes were blocked in PBS + 5% Marvel Milk powder for 1 h. Membranes were then incubated with primary antibody (see table) overnight followed by three 10 min washes in PBS, a 1 h incubation with

secondary antibody (see table) and three 10 min washes in PBS. 0.6 mL luminol reagent +
0.6 mL peroxide solution (Millipore) was then added to each membrane followed by a 1 min
incubation, blotted dry and wrapped in cling film. The cling film-wrapped membranes were
taped into cassettes and autoradiography film (UltraCruz) was placed in the cassette
following by incubation in developer solution (Structurix), washed in tap water and incubated
in fixer solution (Structurix).

Lysis and fractionation

Cells in 6-well plates were kept on ice and washed x2 in PBS. Then 100 µl 1X RIPA buffer +
1:200 PMSF, 1:1000 β-mercaptoethanol and 1:200 protease inhibitor cocktail was added.
The cells were removed with a cell scraper and pipetted into 1.5 ml Eppendorf tubes on ice.
The cells were left on ice for 10 min and then spun in a microcentrifuge at 13,000 g for 10
min. The supernatant was removed to a new tube and the same volume of Laemmli buffer
was added. The pellet was resuspended in 50 µl of Laemmli buffer. For the commercial kit-
based fractionation, B104 cells were grown in DMEM 10% FCS 1% penicillin/streptomycin in
T75 flasks until confluent. The confluent flask was then split into three 10 cm dishes. The
following day, the media in each dish was replaced with 2.5 mL DMEM, 10% FCS, 1%
penicillin/streptomycin 1 h prior to transfection. 15 µL per dish of the PolyJet transfection
reagent, from SignaGen, was diluted in 250 µL DMEM per dish, pipetted up and down four
times, and then immediately added to 5 µg of each DNA construct per dish also diluted in
250 µL DMEM per dish. Following 10 min of incubation at room temperature, the PolyJet-
DNA complexes were dispensed dropwise onto each dish. The media was changed the next
day with 5 mL of DMEM 10% FCS 1% penicillin/streptomycin. The Qproteome Cell
Compartment Kit (cat#: 37502; Qiagen) was used according to the manufacturer's
instructions to fractionate the cells into cytosol, membrane, nucleus, and cytoskeleton
fractions. These fractions were then separated on SDS-PAGE and analysed by Western
Blot.

3 Results

3.1 Bioinformatic analysis of the neuronal splice variants of Enah and Src

Given that rat N1-Src preferentially binds rat N-Enah while rat C-Src has no preference for N-Enah over rat Enah (West et. al., 2019), I hypothesised that the N1-Src microexon co-evolved with the neural exon of N-Enah. I carried out multiple sequence alignments from a variety of animal species from mammals to basal metazoan phyla. The EVH1 domain is the most highly conserved region of the Ena/VASP proteins (Gertler et al., 1996). The EVH1 domain is found conserved in metazoan species most distantly related to mammals (Figure 4A). This suggests that the first protein with an EVH1 domain emerged very early in the evolution of metazoa (animals). The most distantly related animal species to mammals that I could find with a neuronal Enah sequence is the Whale Shark (Figure 4B), which is a cartilaginous fish. This places the emergence of the EVH1-domain-containing protein to around the time the first nervous systems evolved 948 MYA (million years ago) (Hedges et al., 2015) and the N-Enah neuron-specific insert to 476 MYA (Hedges et al., 2015). Given that Ctenophores possess a neural net, neurons may have emerged very early in metazoan evolution; and sponges and placozoans may have evolved to lose their neurons (Ryan and Chiodin, 2015).

(Lewis et al., 2017) carried out an alignment of N1-Src microexon sequences (Figure 5A), which revealed that the cartilaginous fish (cat sharks) also share this neural isoform. The emergence of both neural isoforms (N-Enah and N1-Src) in early chordates is consistent with the current understanding of the evolution of central nervous systems. The presence of conserved tyrosine residues of the neural insert of N-Enah from mammals to cartilaginous fish (Figure 4C) supports the hypothesis that N-Enah evolved with the protein tyrosine kinase N1-Src.

However, it is currently unclear what additional functionality the neuronal exons confer on their respective genes that are important for nervous system function. Phylogenetic trees have been used to visualise the co-evolution of chemokines and chemokine receptors (Goh et al., 2000). Similarly, amino acid sequences of N-Enah and N1-Src, containing their respective neural inserts, from various animal species were used to produce phylogenetic trees (Figure 5B). The similarity of the grouping of species is consistent with these neural sequences having evolved together, but more in-depth analysis would be required to add weight to this hypothesis.
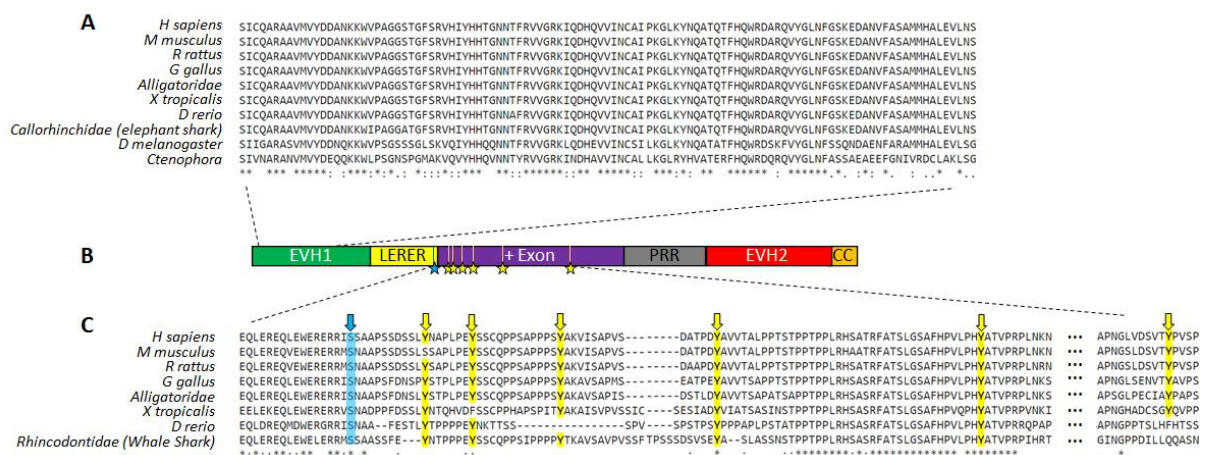
Figure 4. Multiple amino acid sequence alignment of proteins homologous to human N-Enah.

A) Most of the EVH1 domain is conserved from Humans to Ctenophores (Comb Jellies). The dotted line shows that the aligned sequences are found in the N-terminal EVH1 domain of Enah.

B) A domain diagram of N-Enah. From the N terminus on the left: EVH1 is the **E**na/**V**ASP **H**omology **1** domain; LERER is the tandem repeat region; + Exon is the neural enriched insert (non-neuronal Enah does not contain a + Exon); PRR is the proline-rich region; EVH2 is the **E**na/**V**ASP **H**omology **2** domain; CC is the coiled coil domain (C terminus).

C) Conserved sequence at the start of the neural-specific exon of N-Enah from Humans to Whale Shark. The dotted line shows where the aligned sequences are found in the domain diagram of N-Enah. An asterisk (*) is a fully conserved amino acid residue across all sequences. Colons (:) are residues that have strongly similar properties and periods (.) are residues that have weakly similar properties. The blue star is the conserved serine (S264 in Humans) shortly before the neural insert. A blue arrow in B points to the conserved serine in the aligned sequences in which is also highlighted blue. The yellow stars are the conserved tyrosine residues of the neural insert and correspond to the yellow arrows in the aligned sequences in B.

A
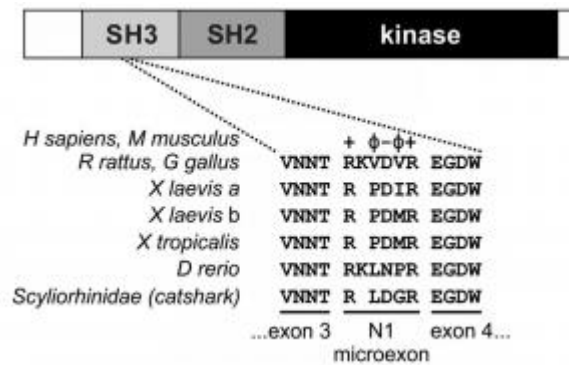
B
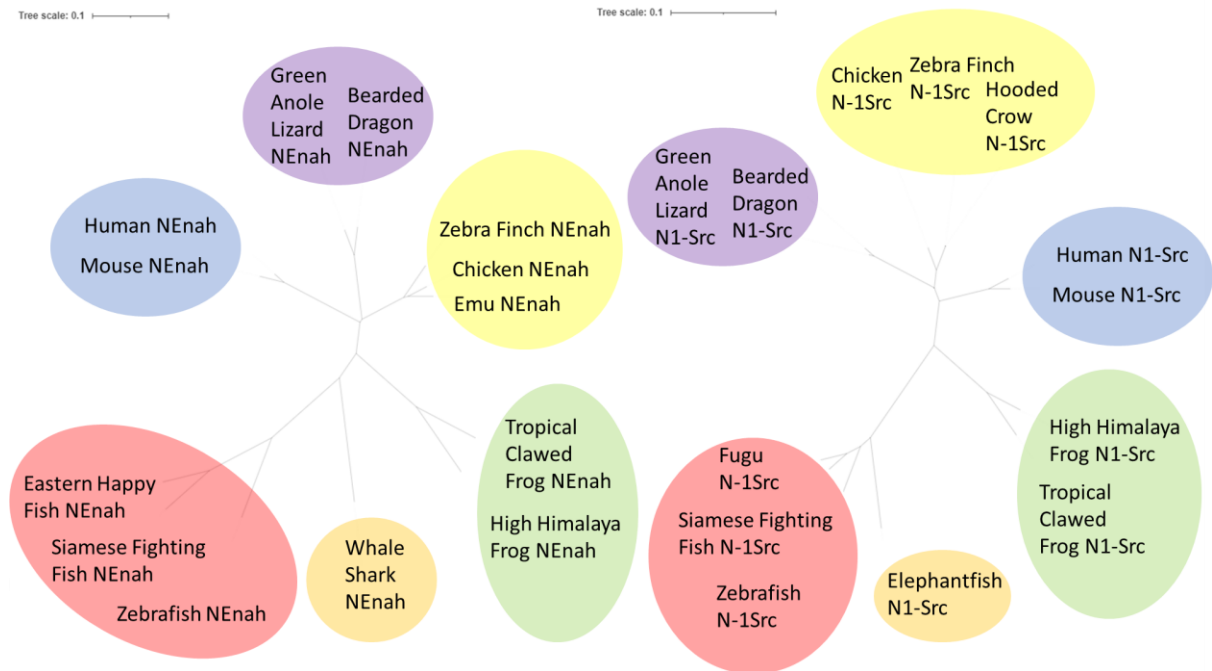
Figure 5. The conserved neural insert of N1-Src (A) and phylogenetic trees of N1-Src and N-Enah (B). A, φ is hydrophobic residue; + is basic residue; - is acidic residue (Lewis et al., 2017).
B, Phylograms of amino acid sequences from various species of mammals, reptiles, birds, amphibians, cartilaginous fish, and bony fish that include the N-Enah neural insert (left) and N1-Src insert (right). Amino acid sequences, acquired from the Ensembl and KEGG genome browsers, were aligned using Clustal Omega to generate tree data which was then visualised in iTOL (interactive Tree Of Life).

3.2 N-Enah-WT, but not N-Enah-6F, is tyrosine phosphorylated in the presence of N1-Src

Given that the tyrosine residues of the neural insert of N-Enah are highly conserved across vertebrates, and N1-Src likely co-evolved with N-Enah, it is possible that N1-Src phosphorylates one or more of these tyrosine residues. One method for investigating whether a protein is tyrosine phosphorylated is to design a mutant that has all putative tyrosine residues mutated to phenylalanine. Phenylalanine is almost identical in structure to tyrosine, differing only in that the hydroxyl group in the ortho position of the benzene ring in tyrosine is replaced with a hydrogen atom in phenylalanine. This hydroxyl group is where phosphate is covalently linked by tyrosine kinases. Such a mutant is therefore 'phosphonull' as it cannot be phosphorylated.

A phosphonull mutant, N-Enah-6F, was designed in which all six tyrosine residues in the neural exon were mutated to phenylalanine (**Figure 6A**). In order to ascertain whether N-Enah is tyrosine phosphorylated by N1-Src, N-Enah-WT, and N-Enah-6F were cotransfected with N1-Src-FLAG in B104 cells and the resulting cell lysates were probed in a phosphotyrosine Western blot **(Figure 6B)**. Enah-mmunoreactive bands migrating at 140 kDa were present in all samples containing overexpressed N-Enah-WT or N-Enah-6F. The 80 kDa bands in the Enah blot most likely represent the broadly expressed (not neuronal-specific) endogenous Enah. In the pY blot, 140 kDa bands were present only in samples containing both N1-Src-FLAG and N-Enah-WT. The only differences between N-Enah-WT and N-Enah-6F are the mutations of six tyrosine residues to phenylalanine and yet this is enough to inhibit phosphorylation of N-Enah in the presence of N1-Src-FLAG.

A

APSSDSSL<mark>Y</mark>SAPLPE<mark>Y</mark>SSCQPPSAPPPS<mark>Y</mark>AKVISAPVSDA
APD<mark>Y</mark>AVVTALPPTSTPPTPPLRHSATRFATSLGSAFHPVL
PH<mark>Y</mark>ATVPRPLNRNSRPSSPVNTPSSQPPAAKSCAWPTSNF
SPLPPSPPIMISSPPGKATGPRPVLPVCVSSPVPQMPPSP
TAPNGSLDSVT<mark>Y</mark>PVSPPPTSGPAAPPPPPPPPPPPPPPPP
PPPLPPLASLSHCGSQASPPPGTPLASTPSSKPSVLPSPS
AA

N-Enah | EVH1 | LERER | + Exon | PRR | EVH2 | CC |

TLM   FAB

B

C

(i)

(ii)

Magnified X3

(iii)

(iv)
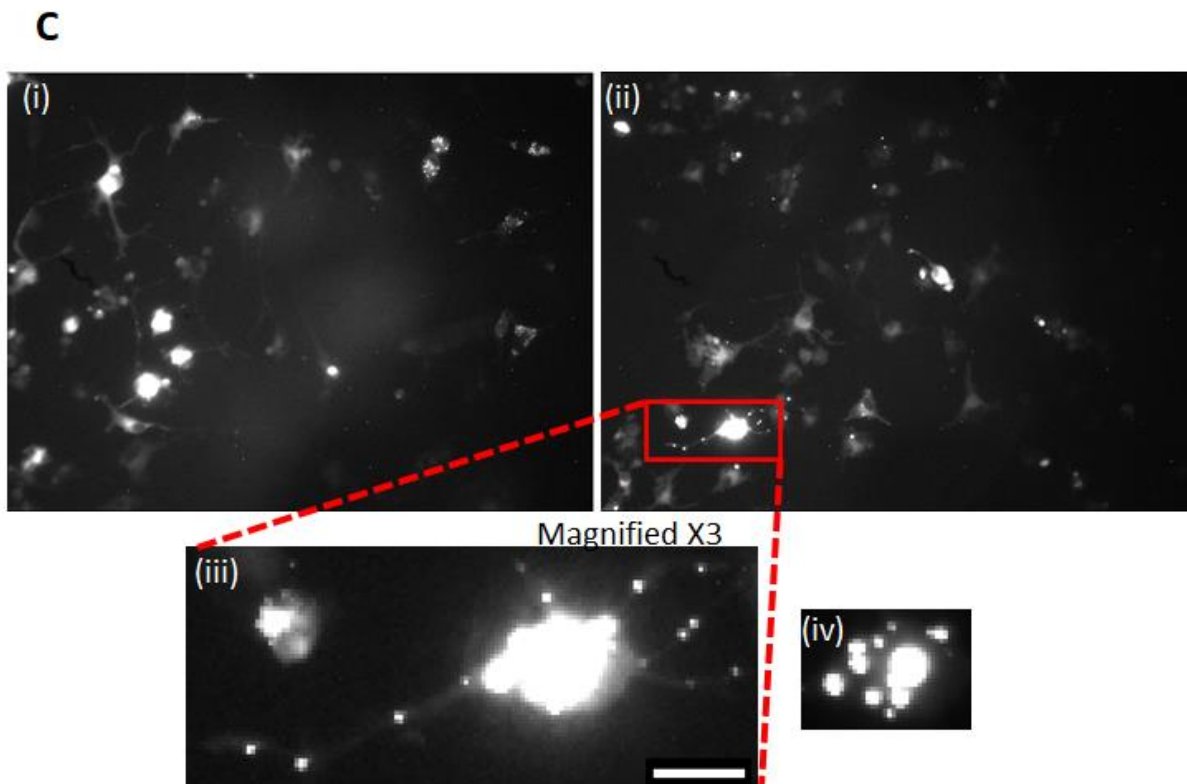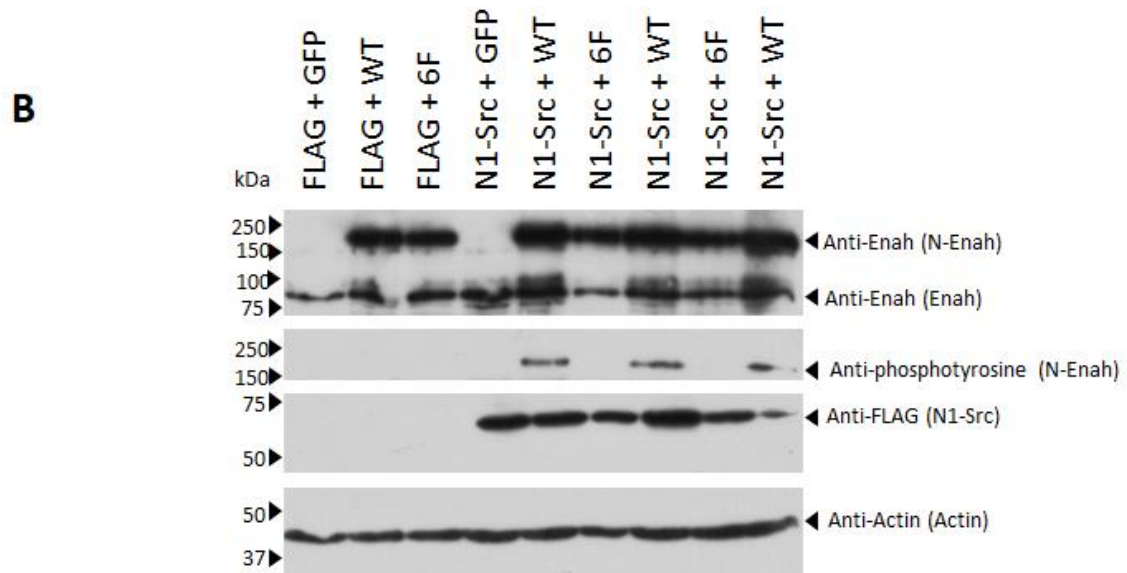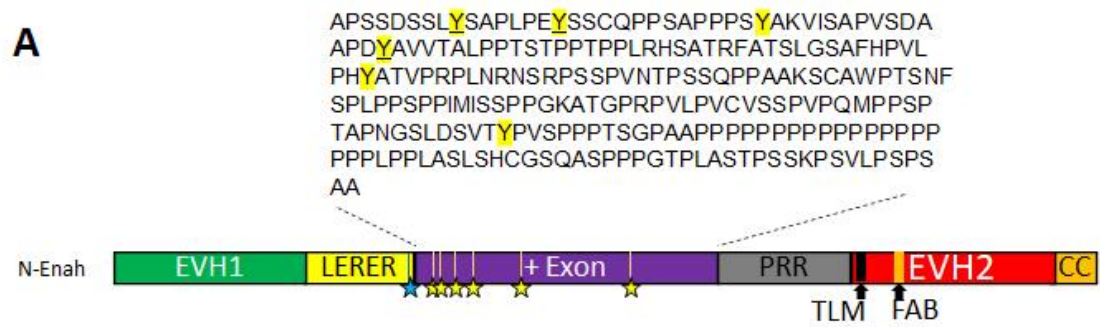
Figure 6 Construction of a phosphomutant GFP-N-Enah plasmid. 1A, Domain diagram of N-Enah showing the 242 amino acid sequence of the neural + exon. The + exon is inserted just after a conserved serine PKA site while another phosphoserine site is found in the TLM and two tyrosine phosphorylation sites are found in the proline rich region. EVH1, Ena/VASP Homology 1 domain. LERER, tandem repeat region with consensus sequence LERER. PRO, proline-rich central core of the protein. TLM, Thymosin-like Motif involved in G-actin binding. FAB, Filamentous Actin Binding domain. EVH2, Ena/VASP Homology 2 domain. The blue star is the conserved serine (S257 in the N-Enah-WT construct). All six tyrosine residues (Y) highlighted yellow are mutated to phenylalanine in N-Enah-6F and are represented as yellow stars in the domain diagram. The three underlined tyrosines in the sequence were identified in MS/MS experiments as binding to N1-Src in previous work by the Evans lab (West et al 2019). **1B,** N-Enah is tyrosine phosphorylated by N1-Src**.** B104 cells were cotransfected with the above constructs for 2.5 days followed by laemmli lysis. The lysates were separated on SDS-PAGE and analysed by Western blot. **1C,** B104 cells transfected with N-Enah-WT (i), and N-Enah-6F (ii) after three days of culture in 2% FCS with 1 mM db-cAMP (dibutyryl cyclic adenosine monophosphate) before being fixed with formaldehyde and mounted with a solution containing DAPI. Section (iii) is magnified X3 and (iv) shows the central cell body of the cell in (iii) but adjusted so the bright punctae can be distinguished. Scale bar is 10 μm.

3.3 Developing a model for neurite outgrowth in which to test the role of N-Enah tyrosine phosphorylation

What is the role of tyrosine phosphorylation of the neural + exon of N-Enah? N-Enah induces membrane protrusions when ectopically expressed in fibroblasts (Gertler et al., 1996) so it is possible that tyrosine phosphorylation regulates membrane protrusion. B104 cells are neuroblastoma cells that, when grown in culture, grow neurites that extend away from the cell body. Overexpression of the phosphonull N-Enah-6F in B104 cells may produce a different morphological phenotype to those overexpressed with N-Enah-WT that could elucidate a function for the tyrosine phosphorylation.

B104 cells are highly heterogeneous. Any difference between overexpression of either construct of N-Enah would likely be lost in the 'noise' of widely varying cell morphology. By inducing the cells to differentiate and develop more and longer neurites, any significant differences would be more likely to be detected.

Retinoic acid (RA) is involved in neuronal differentiation and can be used to treat neurodegeneration and to induce neuron differentiation (Maden, 2007). N^6,O^{29}-dibutyryl-cyclic AMP is membrane permeable and does not activate PKA, however, upon hydrolysis of the 2'-butyrate bond within the cell, the compound becomes a potent activator of PKA (Schwede et al., 2000). The control condition was chosen to be 10% FCS in DMEM as this is the normal growth media used for these cells. The differentiating condition was decided to have a lower serum concentration at 2% FCS in DMEM with the addition of either 1 mM dibutyryl cyclic adenosine monophosphate (db-cAMP), 5 μM retinoic acid (RA), or 1 mM db-cAMP + 5 μM RA.

In order to decide which drug or drug combination to use in the later neurite morphology experiments, B104 cells plated 2.5 x 10^4 cells on 13 mm glass coverslips in 24-well plates were grown with either no drug, 1 mM db-cAMP, 5 μM RA, or 1 mM db-cAMP + 5 μM RA in either 10% FCS in DMEM or 2% FCS in DMEM. The cells were also transfected with pSUPER-EGFP to more easily visualise them. Cells were fixed three days after plating and viewed with a fluorescence microscope set to 285 nm. Micrographs were analysed with the NeuronJ plugin for the ImageJ software.

All cells grown in 2% FCS had significantly more and longer neurites than those grown in 10% FCS. Cells grown with 1 mM db-cAMP in 2% FCS had the most significantly longer neurites than 5 μM RA in 2% FCS, or 1 mM db-cAMP + 5 μM RA in 2% FCS when compared to 10% FCS with no drug (**Figure 8**).

Representative images can be seen in **Figure 7** of each of these conditions tested. The cells grown in 2% FCS and the cells grown in 1 mM db-cAMP do appear to have longer and more numerous neurites. The goal of this preliminary experiment was to optimise the differentiating conditions to be later used in a morphology experiment. Therefore, this

experiment was only conducted once with 30 cells analysed per condition. Such a cell morphology experiment may help to elucidate some possible functions of N-Enah tyrosine phosphorylation. Furthermore, the links between PKA phosphorylation and Ena/VASP regulation in neurons (Lebrand et al., 2004) and the effect of VASP phosphorylation by PKA and the reduction of Abl binding (Howe et al., 2002) and actin binding (Harbeck et al., 2000) support the use of cAMP.

10% FCS in DMEM   2% FCS in DMEM

1 mM db-cAMP

1 mM db-cAMP + 5 µM RA

5 µM RA

Control
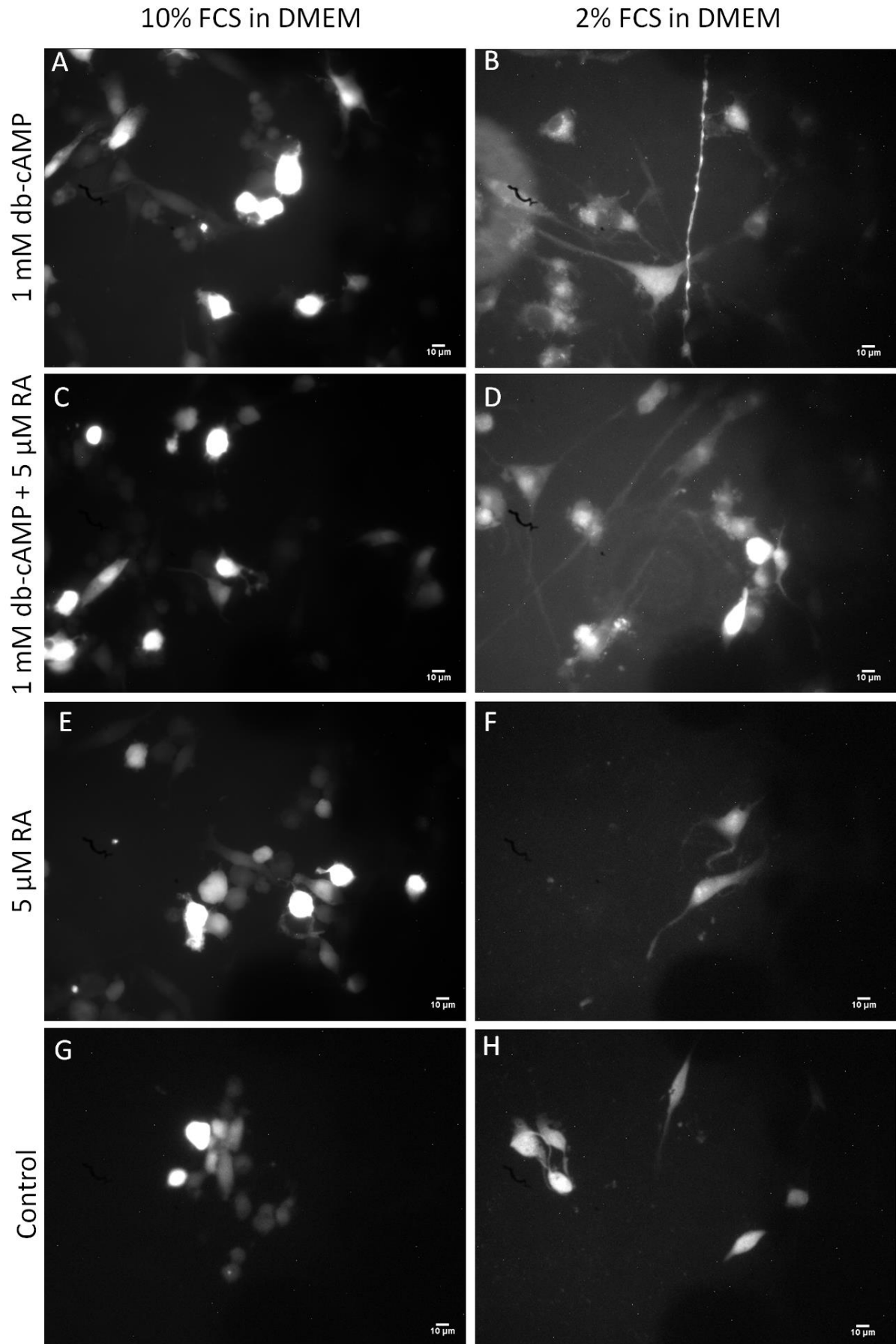
Figure 7. 1 mM db-cAMP with 2% FCS in DMEM is an effective differentiating condition. 2.5 x 10^4 B104 cells were plated on 13 mm coverslips and grown in either 10% FCS in DMEM (A, C, E, and G) or 2% FCS in DMEM (B, D, F, and H). Scale bar 10 μm. The reduction in serum concentration from 10% to 2% reliably increases neurite length (p = 0.007), total neurite length per cell (p = 0.009), total neurites per cell (p = 0.006), and the fraction of cells expressing neurites (p = 0.033). Of the cells grown in 2% FCS in DMEM, those grown in 1 mM db-cAMP, but not cells grown in 1 mM db-cAMP + 5 μM RA, had significantly more total neurites per cell than cells grown in 5 μM RA (p = 0.020). Of all the drugs tested, a significantly greater fraction of the cells grown without any drug (Control) were expressing at least one neurite compared to cells grown in 5 μM RA (p = 0.041). The data were analysed by two way anova followed by Tukey post-hoc test.
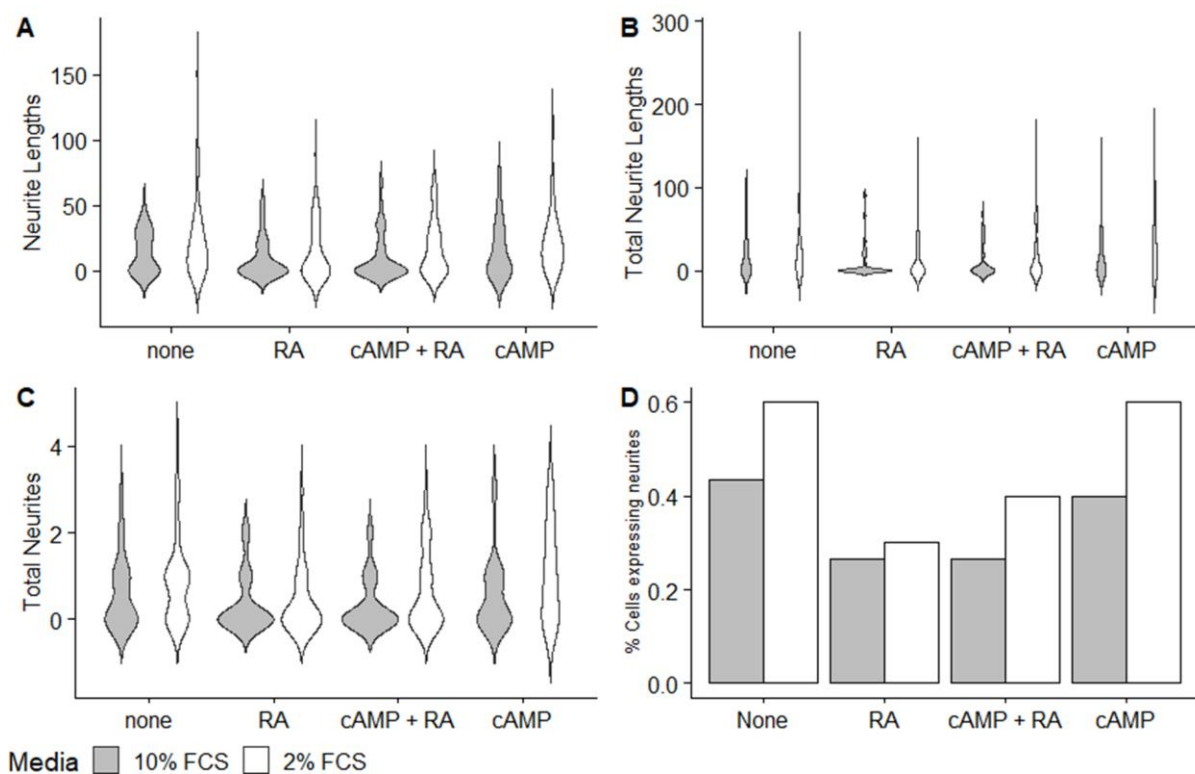
Figure 8. The effect of cAMP, retinoic acid (RA) and reduced serum concentration on morphological differentiation of B104 cells. B104 cells, 2.5 x 10^4, were plated onto 13 mm coverslips before being transfected a day later with a GFP plasmid. The media was replaced the following day with either 2% FCS or 10% FCS and containing either no drug, 5 μM RA, 1 mM db-cAMP + 5 μM RA, or 1 mM cAMP. **A**, a measure of the lengths of all neurites in each condition. **B**, a measure of the total neurite lengths per cell in each condition. **C**, a measure of the total number of neurites per cell in each condition. **D**, the fraction of cells expressing neurites in each condition. This experiment was performed once and 30 cells were analysed for each experimental condition.

3.4 GFP-N-Enah-WT or GFP-N-Enah-6F puncta are similar in size and number

Bright puncta of fluorescence at 285 nm were observed in the N-Enah-WT and N-Enah-6F transfected cells (**Figure 6C (i-iv) and Figure 9**). The bright spots had previously been reported (West et. al., 2019) and are now being reported again for the same construct, N-Enah-WT, in addition to the new phosphonull mutant from this project, N-Enah-6F. Ena/VASP proteins are known to tetramerise (Bear and Gertler, 2009) and Enah has been observed to localise to focal adhesions via the N-terminal EVH1 domain (Gertler et al., 1996). The leading, protruding edge of lamellipodia and filopodia tips are also locations where Enah is found (Applewhite et al., 2007). However, These spots are typically seen throughout the cytosol of the cells (**Figure 6C (i-iv)**).

The puncta were quantified in B104 cells transfected with either of the two N-Enah constructs in both media conditions and two way Anova followed by a Tukey post-hoc test was performed (**Figure 10A**). Quantification was carried out using the SpotCounter plugin for ImageJ. Cells grown in 2% FCS + 1 mM camp did have significantly fewer puncta (P value 0.012). There was no significant difference between the number of puncta of N-Enah-WT transfected cells grown in 10% FCS vs N-Enah-WT grown in 2% FCS + 1 mM cAMP but there was with N-Enah-6F (P value 0.034, **Figure 10A**).
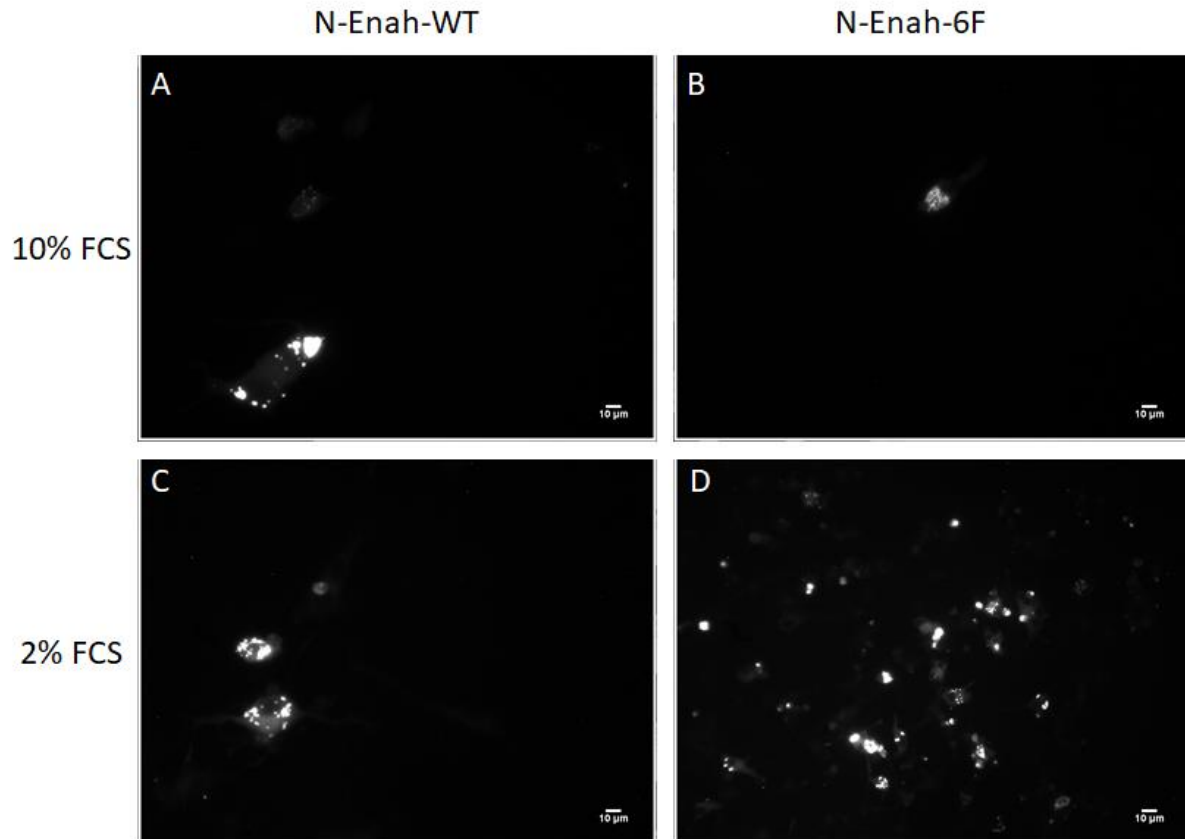
Figure 9. Observations of GFP fluorescence puncta. B104 cells were transfected with N-Enah-WT (A and C), and N-Enah-6F (B and D). After three days of culture in either 10% FCS (A and B) or 2% FCS + 1 mM db-cAMP (C and D) the cells were fixed with formaldehyde and mounted with a solution containing DAPI. GFP Fluorescence puncta were observed in all conditions tested but not in all cells.

As the results for the puncta quantification experiment differed between N-Enah constructs, the experiment was repeated. In this repeat, the SpotCounter plugin was used on GFP transfected cells in addition to those transfected with N-Enah-WT and N-Enah-6F (**Figure 10B**). The presence of data for the GFP cells confirmed suspicions that background noise contributed to the puncta quantification. N-Enah-WT and N-Enah-6F cells both had significantly more puncta than GFP cells (P values <0.001 and 0.009, respectively). However, neither N-Enah construct had a significantly different number of puncta between the different media conditions.

In one last attempt to investigate the puncta of N-Enah transfected cells, the SQUASSH plugin for ImageJ was used to measure the size of puncta in these cells (**Figure 10C**). A two way analysis of variance test determined that there was no significant interaction between N-Enah construct and media the cells were grown in.
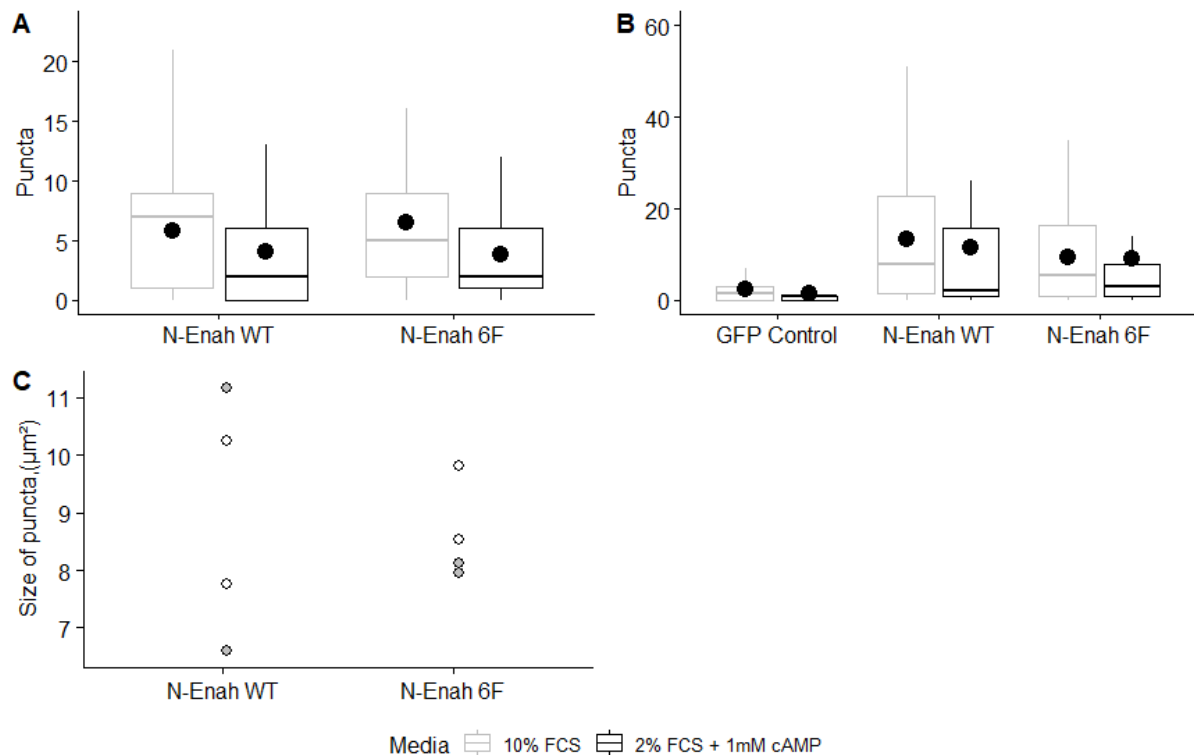
Figure 10. Phosphonull N-Enah-6F does not form more or larger punctae than N-Enah-WT. A, B104 cells transfected with N-Enah-WT, or N-Enah-6F were fixed after 4 days in 10% FCS (grey) or 2% FCS + 1 mM db-cAMP (white) and photos were taken with a fluorescence microscope. The SpotCounter plugin for the ImageJ software was used to quantify the number of puncta and the results were plotted in R Studio. N-Enah-6F did have significantly fewer puncta in 2% FCS + 1 mM cAMP compared to 10% FCS (P value 0.034). **B,** The same experiment as in **A** but with the GFP cells analysed as a measure of background noise. No significant differences were observed between the means in each group. Means are shown as black dots in **A** and **B**. **C,** The SQUASSH plugin for ImageJ was used to analyse two pictures each of N-Enah-WT and N-Enah-6F transfected cells grown in 10% FCS and 2% FCS + 1 mM cAMP. There is no statistically significant interaction between N-Enah construct and puncta size.

3.5 N-Enah-6F is more stably associated with the cytoskeleton than N-Enah-WT

Regulation of cytoskeletal regulators provides the exquisite control necessary for rapid responses to guidance cues. In a cosedimentation assay, VASP, phosphorylated by PKA and incubated with prepolymerised actin, bound to less actin than did wild type VASP (Harbeck et al., 2000). Serine phosphorylation can therefore regulate actin regulators by affecting their affinity for F-actin. V-Src expression in PC12 cells caused an increase in protein tyrosine phosphorylation and neurite extension (Cox and Maness, 1991).

Does tyrosine phosphorylation of the neural + exon of N-Enah affect its association with F-actin in a similar way to PKA-dependent phosphorylation of VASP? To answer this question, and to test whether N-Enah-6F was more stably associated with the cytoskeleton than N-Enah-WT, native lysis was carried out and analysed by Western blotting alongside laemmli lysis (**Figure 11A-B**). Cells were lysed in RIPA lysis buffer and the resulting supernatant and pellet were run on a SDS-PAGE alongside cells lysed with Laemmli buffer. The lysates were transferred from gel to PVDF membrane for analysing by Western blot (**Figure 11A-B**). It appears that there may be more N-Enah-6F in the RIPA-insoluble fraction than with N-Enah-WT.

RIPA lysis buffer was chosen because it would be expected that the cytoskeleton and cytoskeleton-associated proteins would be confined to the insoluble fraction, and not the supernatant, after centrifugation. Indeed, cytoskeletal proteins have been shown to be relatively insoluble in RIPA lysis buffer compared to a urea-based buffer (Ngoka, 2008). However, the same study concluded that cytoskeleton-associated proteins are solubilised in RIPA lysis buffer. Furthermore, proteins with molecular weight greater than 100 kDa may not solubilise in RIPA lysis buffer. However this is an average of the molecular weights of proteins that dissolved in RIPA lysis buffer so the interaction state between the 140 kDa N-Enah (and N-Enah-6F) protein with the actin cytoskeleton may well be preserved in the pellet fraction following RIPA lysis.

For a more defined subcellular fractionation, a commercial kit that generates cytosol, membrane, nucleus and cytoskeletal fractions was employed. Thus, the cellular distributions of overexpressed GFP-N-Enah-WT and GFP-N-Enah-6F could be more accurately determined compared to the RIPA lysis experiment. The results from this kit can be seen in **Figure 11 C-E**. N-Enah-6F (6F) appears to be more strongly associated with the cytoskeleton fraction than does N-Enah-WT (WT).
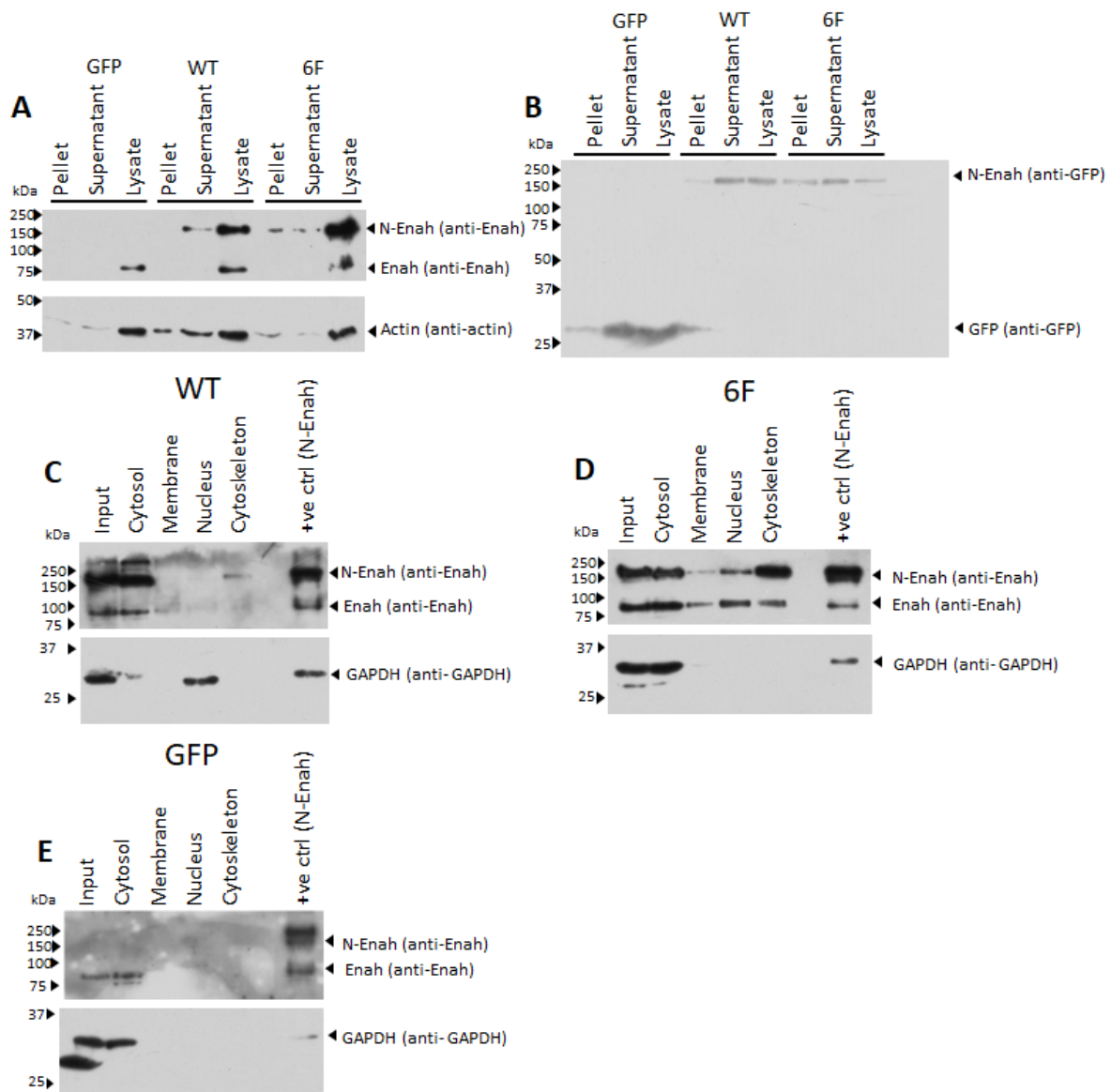
Figure 11 N-Enah-6F is more stably associated with the cytoskeleton than N-Enah-WT. A-C, three separate experiments where B104 cells were transfected with either GFP, N-Enah-WT, or N-Enah-6F and lysed 2.5 days later. Half the wells were lysed by laemmli lysis, Lysate (L) and the other half by RIPA lysis giving Pellet (P) and Supernatant (S) fractions. **D-E**, two separate experiments in which B104 cells

were plated in 10 cm dishes and transfected with N-Enah-WT, N-Enah-6F, or GFP, respectively.

3.6 A phosphonull mutant of N-Enah inhibits the db-cAMP-dependent initiation and extent of neurite outgrowth

Neurite initiation marks the beginning of neuronal morphogenesis as spherical nascent neurons begin to polarise, forming the structural circuitry of the nervous system. A dynamic actin cytoskeleton is a requirement for neurites to form, changing configuration in response to guidance cues (Flynn, 2013). Therefore, actin regulators, such as Enah, play important roles in the structural mechanics of neurite initiation. Increasing phosphorylation of VASP by increased incubation time with PKA led to a reduction of the amount of VASP associated with actin as well as a reduction in actin bundling (Harbeck et al., 2000). Thus phosphorylation is an example of regulation of actin regulators and so may contribute to neurite initiation.

The phosphonull N-Enah-6F mutant was designed such that the tyrosine residues of the neural exon of rat N-Enah were changed to phenylalanine. A possible function for the phosphorylation of these tyrosine residues could therefore be investigated.

In order to determine whether this neural-specific exon is involved in neurite initiation or outgrowth, B104 cells were transfected with either N-Enah Wild Type (N-Enah-WT), a phosphonull mutant N-Enah (N-Enah-6F), or GFP control. Cells were either treated with 10% FCS in DMEM - the non-differentiating condition - or with 2% FCS in DMEM with 1 mM db-cAMP - the differentiating condition. After 4 days, the cells were fixed and images were taken with a fluorescence microscope. There was a significant difference between the non-differentiating condition and the differentiating condition as reported in 2.3.

Fluorescence images of the cells were used to analyse the differences in four parameters. As there were three replicates of this experiment, data had to be normalised in order to combine all the data for statistical analysis. Normalised neurite length (**Figure 12A**) is the length of each neurite measured expressed as a fraction of the the longest neurite measured for that construct (GFP, N-Enah-WT, or N-Enah-6F). Normalised total neurite length per cell (**Figure 12B**) is a measure of the total length of all neurites on each cell, normalised with respect to the maximum values measured for that construct (GFP, N-Enah-WT, or N-Enah-6F). Many cells in all conditions tested had no neurites but were counted in this parameter as it is a measure of the total effect that each cell exerted into differentiating from a spherical cell into a highly polarised cell with processes. Total neurites per cell (**Figure 12C**) is also a measure of differentiation as is the normalised total neurite length per cell parameter and so the cells with no neurites are included as zeroes as those cells have not differentiated beyond a simple shape. The final parameter measured in this experiment, fraction of cells expressing neurites (**Figure 12D**), is also an attempt to elucidate the extent of neurite initiation. Neurite initiation marks the start of the morphological processes, involving the regulated rearrangement of the cytoskeleton, that ultimately defines the structure and function of a neuron in the development of a healthy brain.
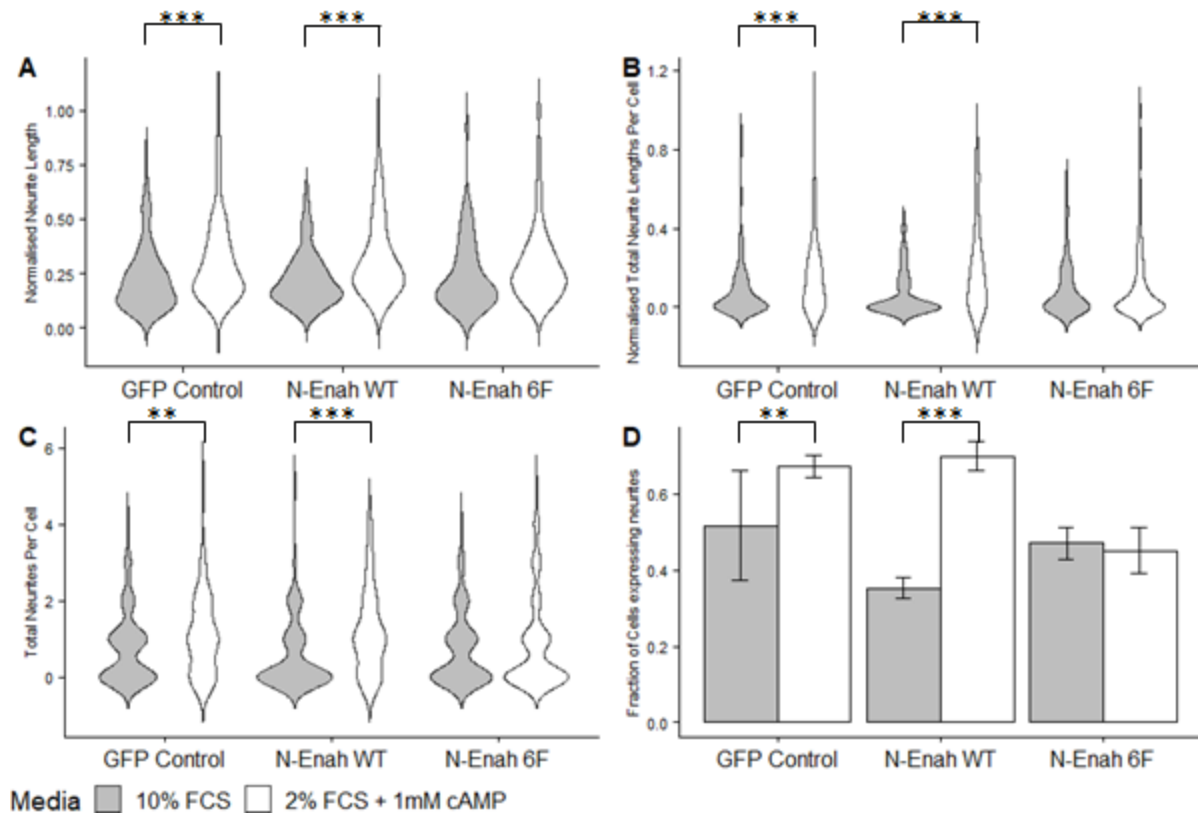
Figure 12. Phosphonull N-Enah-6F suppresses the enhancing effect of db-cAMP on neurite initiation and outgrowth. A, normalised neurite length. **B**, normalised total neurite length per cell. **C**, total number of neurites per cell and **D**, the percentage of cells expressing neurites. B104 cells transfected with GFP, N-Enah-WT, or N-Enah-6F were fixed after 4 days in 10% FCS (grey) or 2% FCS + 1 mM db-cAMP (white) and photos were taken with a fluorescence microscope. Neurite lengths were measured with the NeuronJ plug-in for ImageJ. For each replicate, neurite lengths were normalised to the maximum neurite length in each condition. Data are plotted as boxplot and are from three independent experiments. Data are mean ± SEM, n=3 individual experiments (≥ 30 cells analysed/condition/experiment). Statistical analysis was performed by two-way ANOVA with pairwise comparisons by Tukey post-hoc test **p<0.01, ***p<0.001.

4 Discussion

This project sought to investigate an interaction between N1-Src and N-Enah and to elucidate a role for tyrosine phosphorylation of N-Enah. N1-Src and N-Enah likely evolved alongside each other with the tyrosines of the N-Enah insert during early vertebrate evolution. The phosphonull N-Enah-6F mutant, with the six tyrosine residues of the neural insert mutated to phenylalanine, was cloned into a GFP-expression plasmid. Following co-expression in neuroblastoma cells with FLAG-tagged N1-Src, N-Enah-6F could not be detected by immunoblotting with a phosphotyrosine antibody while N-Enah could. The 6F mutant was also found to be more stably associated with the cytoskeleton through the use of cell fractionation experiments. A cAMP-dependent effect on neurite outgrowth was inhibited by N-Enah-6F expression. This confirms the hypothesis that tyrosine phosphorylation by N1-Src is important in regulating the interactions of this actin regulator with other proteins necessary for its functions in processes such as axon guidance.

4.1 N-Enah and N1-Src evolved together

N-Enah and N1-Src are alternate splices of Enah and Src, respectively, and are enriched in neurons (Maness et al., 1988; Gertler et al., 1996). The alternative splicing (AS) of genes has been proposed to contribute to complexity in higher eukaryotes (Chen et al., 2012). Animals have more AS than plants and vertebrates have more AS than invertebrates (Chen et al., 2012). Primate species were found to have higher alternative splicing levels (ASLs) than other vertebrate species (Barbosa-Morais et al., 2012). Organ-dependent mRNA expression is conserved through vertebrates whilst AS may have been more important for shaping species-specific differences. ASLs can even be used to predict the complexity of a species as more complex organisms usually have more alternative splicing (Iñiguez and Hernández, 2017).

So if an increase in alternative splicing can help explain the increased complexity of higher eukaryotes, and human brain tissue has a higher prevalence of alternative splicing than other tissues, neural splice variants such as N-Enah and N1-Src could have emerged at the same time. In **Figure 4**, the amino acid alignments of Enah from a variety of animal species shows that the EVH1 domain is conserved in some of the most basal of metazoan phyla (Ctenophores) while the neural N-Enah insert and its tyrosine residues are found only from mammals to cartilaginous fish (Whale Sharks). As the N1-Src insert is also found in species spanning the vertebrate subphylum, this is consistent with N1-Src and N-Enah having evolved together. However, at this stage, the evidence is circumstantial and requires further investigation.

An approach was taken to visualise N-Enah and N1-Src evolution together using phylogenetic trees (Figure 5B). Initially, the amino acid sequences acquired from genome browsers produced phylogenetic trees that were not consistent with animal evolution. This was likely due to the presence of alternative splicing of N-Enah in which there are two alternative exons in addition to the large + exon. A decision was then made to focus only on the sequences that are neuronal-specific. The results of this phylogenetic analysis are two strikingly similar phylogenetic trees. Nevertheless, the subjectivity in the grouping of species and the arbitrary manner of choosing the sequences to compare cannot be denied.

4.2 N-Enah is tyrosine phosphorylated by N1-Src

The presence of signal at 140 kDa in the phosphotyrosine blot in Figure 6 confirms work carried out by West et al. The fact that this band is not present when the phosphonull N-Enah-6F is cotransfected with N1-Src hints that at least one of the mutated tyrosine residues are target phosphorylation sites for N1-Src. An immunoprecipitation assay with GFP as bait prior to Western blotting for phosphotyrosine would confirm that the 140 kDa phosphoprotein is indeed GFP-N-Enah. Preliminary work by the Evans lab involved screening for SH3

ligands and substrates of C-Src and N1-Src, using SH3-pulldown assays or *in vitro* kinase

assays followed by mass spectrometry (West et. al., 2019). Three of the peptides identified

by mass spectrometry were tyrosine phosphorylated and unique in sequence to N-Enah.

This is further evidence that these three tyrosine residues (Y280, Y287, and Y315 of human

N-Enah) are substrates for N1-Src.

There is an absence of phosphotyrosine reactive signal at 80 kDa, corresponding to tyrosine

phosphorylation of endogenous Enah, in the cotransfection experiment (**Figure 6B**)

However, there is evidence that Enah is phosphorylated by Abl at Y296 (Tani et al., 2003).

This apparent contradiction can be explained as a sensitivity issue. Any mono-

phosphorylation of endogenous levels of Enah could be dwarfed by the processive tyrosine

phosphorylation of overexpressed N-Enah. It could also be that phosphorylation of Y296 by

Abl is a transient step followed by dephosphorylation. Or even that this phosphorylation

event doesn't occur naturally given that this was only demonstrated in T293 cells

overexpressed with c-Abl, GST-tagged Enah, and FLAG-tagged Abi-1 (Tani et al., 2003).

4.3 N-Enah overexpression in B104 cells does not stimulate neurite outgrowth

The overexpression of genes in cell culture is a common technique for investigating the

function of genes. Fortunately for genes involved in cell morphology, even a subtle

phenotype may be identified following accurate measurements and stringent statistical

analyses. As N-Enah is an actin regulator, this study incorporated a cell morphology

experiment with the expectation that N-Enah overexpression would have a significant impact

on the length or number of measured neurites. Furthermore, ectopic expression of N-Enah in

RAT2 fibroblasts elicited membrane protrusions that contained overlapping N-Enah

immunoreactivity with high concentrations of F-actin (Gertler et al., 1996). It is surprising that

there was no significant difference between the GFP, GFP-N-Enah and GFP-N-Enah-6F

constructs of the cells grown in 10% FCS in all four neurite parameters measured. This

result suggests that N-Enah overexpression in B104 cells has no significant effect on neurite length, number of neurites per cell, total neurite length per cell, or the fraction of cells expressing neurites. However, N1-Src overexpression in cerebellar granule neurons also did not stimulate neurite outgrowth while ectopic N1-Src overexpression in COS7 fibroblasts did lead to the production of membranous protrotrusions (Keenan et al., 2017). Inhibition or knockdown of N1-Src inhibits neurite outgrowth, so too much or too little N1-Src seems to have a negative effect on neurite outgrowth in neurons (Keenan et al., 2017). N1-Src and N-Enah therefore have consistent effects in fibroblasts and neuronal cells. These neural isoforms both stimulate membrane protrusions when ectopically expressed in fibroblasts but are more tightly regulated in neurons where they are naturally found. Therefore, it is the regulation of these proteins that determines their functions in neurons. Tyrosine phosphorylation is one likely mechanism for regulating their function by affecting interactions with other proteins.

The hypothesis of this project postulates that phosphorylation of N-Enah affects the binding of other proteins to this actin regulator. In this project, the overexpression of N-Enah did not produce a morphological phenotype in neuroblastoma cells (**Figure 12**). If regulation of N-Enah is required for normal function, simply overexpressing N-Enah may not be enough to produce a morphological phenotype. Transfection is not the only method to overexpress a gene. Several studies have relocalised all Ena/VASP proteins in order to overexpress or knock down Ena/VASP function. An approach that sequesters all Ena/VASP proteins to either mitochondria, cell membranes, or to the cytosol has been used extensively to silence or potentiate Ena/VASP function. When expressed in eukaryotic cells, ActA peptide from the intracellular pathogen Listeria monocytogenes localises to the mitochondrial membrane via the C-terminus (Pistor et al., 1994) and interacts with the actin-nucleating Arp2/3 complex (Bear et al., 2000). A construct was created in which ActA, fused to EGFP and missing the N-terminal Arp2/3 binding domain but containing four repeats of the EVH1 binding motif FPPPP, FP4-mito, has been shown to sequester Ena/VASP proteins to the mitochondrial

surface (Bear et al., 2000). Relocalisation of Ena/VASP proteins away from the actin-rich lamellipodia of fibroblasts caused an increase in cell speed (Bear et al., 2000). This result may at first seem paradoxical as Ena/VASP proteins promote actin filament elongation and inhibit actin capping proteins that would otherwise halt F-actin polymerisation (Kwiatkowski et al., 2003). Furthermore, the protrusion rate of lamellipodia in B16 cells is positively correlated with GFP-VASP concentration (Rottner et al., 1999). An explanation for this paradox emerges from the observation that cell motility is dependent on more than just membrane protrusion. Protruding lamellipodia need to also stabilise these protrusions, adhere to the extracellular matrix, and contract actin filaments to translocate (Bear et al., 2002). This may help to explain how the overexpression of N-Enah-WT did not increase neurite parameters with respect to the GFP control (**Figure 12**). Phosphomutants of Enah have been used to probe fibroblast motility. The conserved PKA site, S236, has been mutated to alanine to prohibit phosphorylation (Loureiro et al., 2002) and to aspartate to mimic phosphorylation (Diviani and Scott, 2001). Fibroblasts lacking Ena/VASP have a hypermotile phenotype. The non-phosphorylatable mutant fails to rescue this phenotype (Loureiro et al., 2002), while the phosphomimetic mutant does slow the hypermotile cells (Diviani and Scott, 2001). Taken together, the studies of Ena/VASP overexpression on fibroblast motility are consistent with my hypothesis. Regulation of N-Enah by modulating its interactions with other proteins is important for its function. Phosphorylation is one example of a mechanism that affects such interactions.

Another construct, FP4-CAAX has the same EVH1-binding motif of FP4-mito but fused instead to a domain within H-Ras that localises to the cell membrane (Bear et al., 2000). In cultured hippocampal neurons, netrin-1 induced the number and length of filopodia in the growth cone (Lebrand et al., 2004). Filopodia length and number were reduced in neurons expressing FP4-mito and increased in neurons expressing FP4-CAAX. Netrin-1 treatment of these neurons induced the formation of lamellipodia and filopodia. However, both FP4-mito-expressing and FP4-CAAX-expressing neurons did not have increased filopodia lengths in

response to netrin-1 treatment although the lamellipodia did still protrude. This netrin-1-induced response was also blocked with the addition of function-blocking anti-DCC antibodies. Taken together, Ena/VASP, PKA, and the netrin-1 receptor DCC were all required for the response of the growth cone filopodia to netrin-1.

Phosphorylation of N-Enah by PKA therefore likely activates Ena/VASP proteins such as N-Enah in vertebrates (Krause et al., 2003) so is early in the N-Enah pathway (**Figure 13A)**.
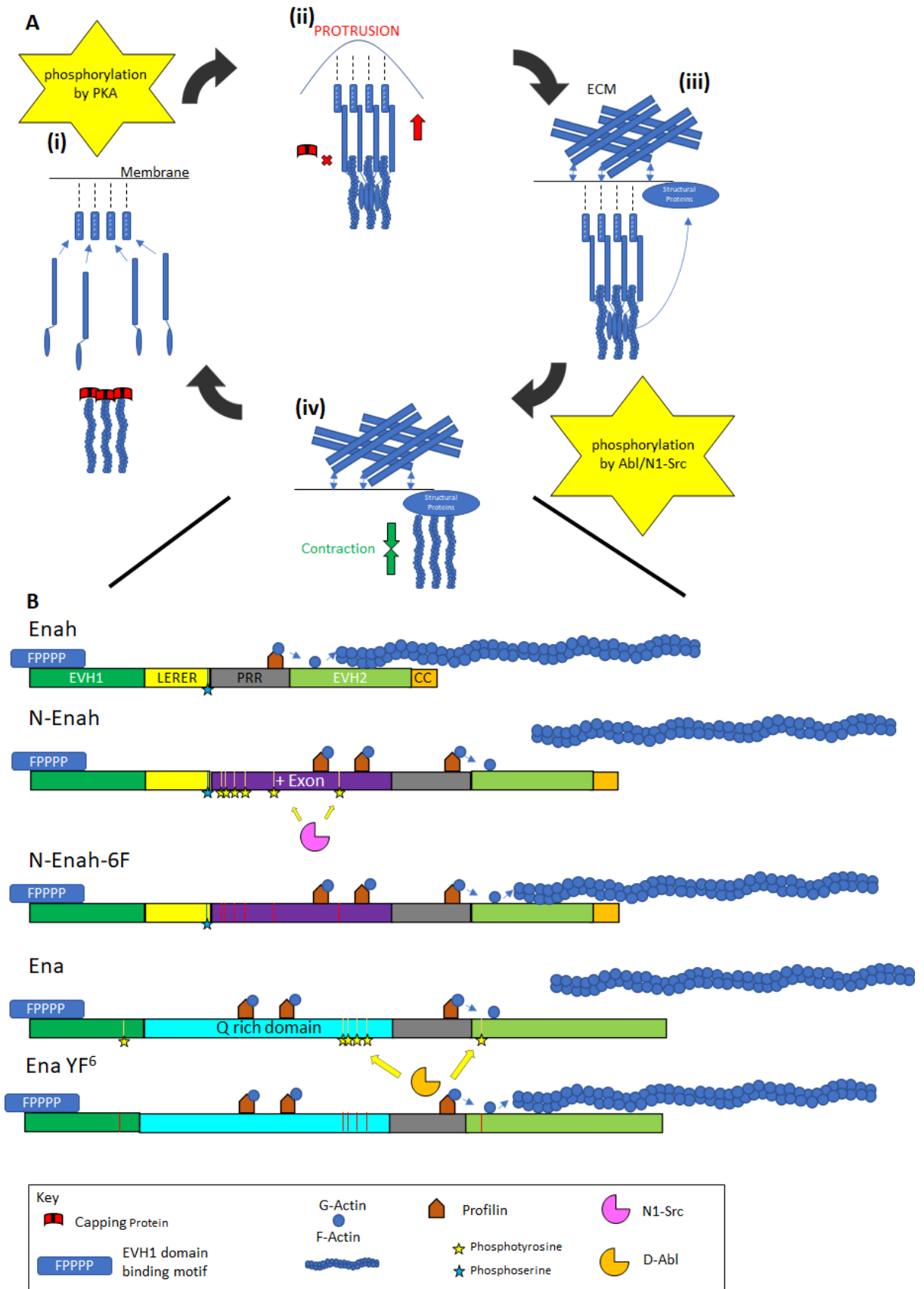
Figure 13. A proposed mechanism of the neural exon of N-Enah. A, a membrane protrusion cycle. **A(i)**, The N-terminal EVH1 domain of Enah binds to proteins containing the 'FPPPP' motif which are associated with the membrane. An actin

filament bundle is capped at the barbed end by capping protein. **A(ii)**, Enah binds actin filaments, displacing and blocking capping protein. Phosphorylation of N-Enah by PKA elevates activity of N-Enah, causing actin polymerisation. **A(iii)**, Connections are made between the extracellular matrix (ECM) and structural proteins embedded in the membrane which in turn are linked to the actin filaments. **A(iv)**, N-Enah undocks from actin filaments following tyrosine phosphorylation. Contraction due to the mechanical force provided by motor proteins such as non-muscle myosin II pulls the F-actin bundle towards the ECM. **B**, Schematics of Enah, N-Enah, N-Enah-6F, Ena and Ena YF[6] with suggested binding partners. The + exon and LERER tandem repeat region of N-Enah recapitulate the Q-rich domain of Ena in that they both contain extra binding sites for proteins that bind proline-rich sequences such as profilin. The tyrosine phosphorylated N-Enah and Ena are shown to be undocked from an actin filament while their phosphomutant counterparts are shown attached to the actin filament.

4.4 N-Enah-6F is more stably associated with the actin cytoskeleton

When N-Enah overexpression is combined with reduced serum concentration (2% FCS) and 1 mM db-cAMP, there is a significant increase in all four neurite parameters measured. Although these effects are also seen in control GFP-transfected cells, these effects are completely ablated when N-Enah-WT is swapped with N-Enah-6F. This suggests that phosphorylation of at least one of the six tyrosine residues mutated to phenylalanine in this study are responsible for the cells' response to the reduced serum concentration and in the presence of 1 mM db-cAMP. It is possible that one or more of these tyrosines are responsible for maintaining the functional structure of the folded protein.

B104 cells solubilised with RIPA buffer and centrifuged were separated into pellet and supernatant fractions. The pellet fractions of cells transfected with N-Enah-6F had greater Enah immunoreactivity compared to the supernatant fraction than did cells transfected with N-Enah-WT (**Figure 11A-B**). The whole-cell lysate fractions, solubilised in Laemmli buffer, had lower Enah immunoreactivity at 140 kDa (the molecular mass of N-Enah) in the N-Enah-6F cells compared to N-Enah-WT cells, suggesting that fewer N-Enah-6F cells were harvested than N-Enah-WT cells, and yet there was still greater immunoreactivity at 140 kDa

in the pellet fractions for N-Enah-6F (**Figure 11B**). A commercial biochemical kit was used to produce a more defined fractionation of cells into cytosolic, membranous, nuclear, and cytoskeletal fractions (**Figure 11**). A more defined fractionation was needed because the RIPA-insoluble fractions of Figure 11A-C could not be proven to represent a specific cytoskeletal fraction. There was observed to be greater Enah immunoreactivity at 140 kDa in the cytoskeletal fraction of N-Enah-6F cells compared to the cytosol fraction (**Figure 11D**) when compared to N-Enah-WT cells (**Figure 11C**). Although the reason for the relative absence of endogenous 80 kDa Enah in the N-Enah-WT experiment is unclear, the presence of endogenous 80 kDa Enah immunoreactivity in the N-Enah-6F blot acts as an internal control. Both 80 kDa immunoreactivity in the N-Enah-6F blot and 140 kDa immunoreactivity in the N-Enah-WT blot had higher cytosolic to cytoskeleton ratios than did immunoreactivity at 140 kDa in the N-Enah-6F blot. Taken together, these experiments further support the idea that N-Enah-6F has higher affinity for the cytoskeleton than does N-Enah-WT or endogenous Enah, and that phosphorylation of the tyrosines in the N-Enah neural insert is a requirement for N-Enah to dissociate from the cytoskeleton. This is consistent with the finding that tyrosine phosphorylation of drosophila Ena by Abl negatively regulates protein-protein interactions (Comer et al., 1998) in which six tyrosines in Ena were mutated to phenylalanine similarly to N-Enah-6F in this project (EnaYF[6] in **Figure 13B**). Tyrosine phosphorylation of N-Enah is likely later in the pathway than PKA phosphorylation and could cause dissociation of N-Enah from F-actin (**Figure 13A**).

There appears to be an up-regulation of endogenous 80 kDa Enah in the presence of N-Enah-WT or N-Enah-6F overexpression as there is an increase in intensity of the 80 kDa bands in the Enah blot of Figure 6. Perhaps the overexpressed N-Enah-WT and N-Enah-6F complex with endogenous 80 kDa Enah through the C-terminal tetramerisation domains. These complexes, which may be related to the punctae seen in the fluorescence images, could protect 80 kDa Enah from proteolytic degradation.

4.5 Phosphonull N-Enah-6F suppresses the enhancing effect of db-cAMP on neurite initiation and outgrowth

A reduction in media serum concentration from 10% to 2% combined with the addition of 1 mM db-cAMP reliably enhances the length of and prevalence of neurites in B104 cells (**Figure 12)**. This enhancement is observed in GFP- and N-Enah-WT-transfected cells but is not seen in cells transfected with the phosphonull N-Enah-6F.

How is it that the tyrosines of the + exon not being phosphorylatable blocks cAMP-dependent neurite outgrowth? The answer might be related to the proximity of the PKA site to the neural + exon. The tyrosines of the + exon are more proximal to the N-terminus of the insert, placing them close to the conserved serine that is phosphorylated by PKA. This serine residue (S236 in mice (Gertler et al., 1996); S265 in human Enah) is highly conserved in all vertebrate Ena/VASP proteins (Kwiatkowski et al., 2003) and is phosphorylated by PKA (Eigenthaler et al., 1992; Gertler et al., 1996; Lambrechts et al., 2000)(Eigenthaler et al., 1992). A Netrin-1 → DCC → PKA → Ena/VASP pathway has already been proposed (Dent et al., 2011). Ena/VASP and PKA are both required for a netrin-1-induced increase in filopodia length and number in cultured hippocampal neurons (Lebrand et al., 2004). The proximity of the PKA site to the six tyrosine phosphorylation sites might indicate an interaction between an axon guidance pathway and regulation of the actin cytoskeleton.

Increasing incubation times of VASP with PKA resulted in a reduction in binding to F-actin (Harbeck et al., 2000). This suggests that PKA may negatively regulate VASP (and possibly N-Enah) activity which contradicts with the notion that PKA activates Ena/VASP proteins (Krause et al., 2003). An actin cosedimentation assay could be carried out for phospho/dephospho N-Enah neural exon and/or full-length N-Enah. The model proposed in **Figure 13** shows N-Enah-6F and Ena-YF[6] bound to F-actin while their wild-type counterparts

are not bound to F-actin as they are tyrosine phosphorylated by N1-Src and D-Abl, respectively.

Future directions

4.6 Dissecting the molecular mechanism of the regulation of N-Enah by N1-Src

Having highlighted the importance of N-Enah phosphorylation in neurite outgrowth using the 6F mutant, work extending from this project should address the molecular mechanisms up- and downstream of N-Enah tyrosine phosphorylation. A first step could be to determine the interactome of phospho- and dephospho-N-Enah to establish the phosphorylation specific protein-protein interactions of N-Enah. A truncated wildtype and 6F N-Enah construct containing the neural insert and the preceding amino acids that include the conserved PKA site, could be used to generate recombinant GST-fusion proteins in *E coli*. If a TKX bacterial strain is used (containing an inducible tyrosine kinase) to express the recombinant proteins, the wildtype construct would be phosphorylated in the bacteria before being purified and this could be compared to the de-phospho form in a GST pulldown assay from neuronal lysates. Binding partners could be identified by immunoblotting for known Enah partners or screening by LC-MS/MS mass spectrometry. Such an experiment could reveal whether PKA only binds to the + exon of N-Enah after it has been tyrosine phosphorylated by N1-Src. Results arising from a pulldown screen could then be followed up in in vitro actin based assays, such as cosedimentation and polymerisation to gain insight into how phosphoregulation of N-Enah binding partners influences actin binding and dynamics (Comer et al., 1998; Harbeck et al., 2000; Chen et al., 2020).

4.7 Phosphoregulation of N-Enah in neurons and the brain

During development, the growth cone is where much of the signal transduction occurs between guidance molecules and the cytoskeleton (Dent et al., 2011). Neurodevelopmental

disorders such as schizophrenia and autism are linked to aberrant formation of neural circuits (Stoeckli, 2018). Clearly, the function and dysfunction of cytoskeletal regulators plays an important role in the health and disease of nervous system development, respectively. It is therefore possible that neuronal splicing of Enah to yield N-Enah and its regulation by N1-Src has as yet undefined roles in these processes.

In order to study the effect of N-Enah and its tyrosine phosphorylation in the growth cone on neurite outgrowth, further work should aim to knockdown N-Enah expression in neurons and rescue with an shRNA-resistant wildtype or 6F phosphonull N-Enah construct (Figure 14, appendix). Having both GFP and Cerulean Fluorescent Protein (CFP) shRNA constructs available would permit flexibility with the use of fluorophores in future co-transfection experiments. pSUPER-GFP-N-Enah shRNA (shRNA1-4) and pSUPER-mCer-N-Enah shRNA (shRNA5-8) plasmids were successfully constructed and confirmed by Sanger sequencing. Co-transfection of the pSUPER plasmids together with the GFP-N-Enah wildtype plasmid confirmed targeting of the shRNA to the N-Enah insert (Figure 14, appendix). Unfortunately there has not been time in this project to further investigate the knockdown of N-Enah in cells, but these promising reagents can be used in future experiments to implicate the tyrosine residues in the N-Enah insert in neurite outgrowth in neurons.

In terms of the impact of N-Enah phosphorylation on nervous system development in the organism, the N-Enah + exon has been observed in the developing mouse nervous system (Lanier et al., 1999). Furthermore, double heterozygous mutant mice embryos lacking Enah and profilin I were observed to be smaller than wild type embryos with aberrant head morphology (Lanier et al., 1999). This experiment in mice embryos should be repeated with the splice-specific knockdown of N-Enah instead of Enah to dissect any specific role of the the + exon in this phenotype. A further, more subtle mouse model in which the + exon is mutated to yield a 6F-N-Enah, perhaps by CRISPR, would definitively address the role of N-

Enah tyrosine phosphorylation in brain development. An inducible version of this model would also allow any developmental aberrations to be distinguished from adult behavioural changes. Although N-Enah has not yet been linked to any human neurodevelopmental or other neurological disorders, the generation of these mouse models would allow such possibilities to be investigated. Furthermore, since N-Enah is a strong driver of actin polymerisation, it is possible the gene could be harnessed or targeted in disorders of nerve growth such as nerve injury (Gertler et al., 1996; Hoyng et al., 2015).

In summary, this project validates work by others showing that phosphorylation of Ena/VASP proteins such as N-Enah regulates interactions with other proteins. These protein-protein interactions may be necessary for functions in actin cytoskeletal remodelling in axon guidance or may exemplify cross-talk between signalling pathways.

References

Sobre la aparición de las expansiones celulares en la médula embrionaria. Gac Sanit Barc 12, 413–419

West LC (2019) "Proteomic and structural analysis of the Neuronal Src SH3 domain" PhD thesis.

Weiss P. Nerve patterns: the mechanics of nerve growth. *Growth, Third Growth Symposium.* 1941;5:163–203

Applewhite DA, Barzik M, Kojima S-I, Svitkina TM, Gertler FB, Borisy GG (2007) Ena/VASP proteins have an anti-capping independent function in filopodia formation. Mol Biol Cell 18:2579–2591.

Barbosa-Morais NL, Irimia M, Pan Q, Xiong HY, Gueroussov S, Lee LJ, Slobodeniuc V, Kutter C, Watt S, Colak R, Kim T, Misquitta-Ali CM, Wilson MD, Kim PM, Odom DT, Frey BJ, Blencowe BJ (2012) The evolutionary landscape of alternative splicing in vertebrate species. Science 338:1587–1593.

Bashaw GJ, Klein R (2010) Signaling from axon guidance receptors. Cold Spring Harb Perspect Biol 2:a001941.

Bate CM (1976) Pioneer neurones in an insect embryo. Nature 260:54–56.

Bear JE, Gertler FB (2009) Ena/VASP: towards resolving a pointed controversy at the barbed end. J Cell Sci 122:1947–1953.

Bear JE, Loureiro JJ, Libova I, Fässler R, Wehland J, Gertler FB (2000) Negative regulation of fibroblast motility by Ena/VASP proteins. Cell 101:717–728.

Bear JE, Svitkina TM, Krause M, Schafer DA, Loureiro JJ, Strasser GA, Maly IV, Chaga OY, Cooper JA, Borisy GG, Gertler FB (2002) Antagonism between Ena/VASP proteins and actin filament capping regulates fibroblast motility. Cell 109:509–521.

Boyer NP, Gupton SL (2018) Revisiting Netrin-1: One Who Guides (Axons). Front Cell Neurosci 12:221.

Brose K, Bland KS, Wang KH, Arnott D, Henzel W, Goodman CS, Tessier-Lavigne M, Kidd T (1999) Slit proteins bind Robo receptors and have an evolutionarily conserved role in repulsive axon guidance. Cell 96:795–806.

Butt E, Abel K, Krieger M, Palm D, Hoppe V, Hoppe J, Walter U (1994) cAMP- and cGMP-dependent protein kinase phosphorylation sites of the focal adhesion vasodilator-stimulated phosphoprotein (VASP) in vitro and in intact human platelets. J Biol Chem 269:14509–14517.

Chen L, Tovar-Corona JM, Urrutia AO (2012) Alternative Splicing: A Potential Source of Functional Innovation in the Eukaryotic Genome. Int J Evol Biol 2012 Available at: https://www.hindawi.com/journals/ijeb/2012/596274/ [Accessed January 10, 2021].

Chen Y, Xu J, Zhang Y, Ma S, Yi W, Liu S, Yu X, Wang J, Chen Y (2020) Coronin 2B regulates dendrite outgrowth by modulating actin dynamics. FEBS Lett 594:2975–2987.

Cohen S (2008) Origins of growth factors: NGF and EGF. J Biol Chem 283:33793–33797.

Comer AR, Ahern-Djamali SM, Juang JL, Jackson PD, Hoffmann FM (1998) Phosphorylation of Enabled by the Drosophila Abelson tyrosine kinase regulates the in vivo function and protein-protein interactions of Enabled. Mol Cell Biol 18:152–160.

Cox ME, Maness PF (1991) Neurite extension and protein tyrosine phosphorylation elicited by inducible expression of the v-src oncogene in a PC12 cell line. Exp Cell Res 195:423–431.

Dent EW, Gupton SL, Gertler FB (2011) The growth cone cytoskeleton in axon outgrowth and guidance. Cold Spring Harb Perspect Biol 3 Available at: http://dx.doi.org/10.1101/cshperspect.a001800.

Diviani D, Scott JD (2001) AKAP signaling complexes at the cytoskeleton. J Cell Sci 114:1431–1437.

Eigenthaler M, Nolte C, Halbrügge M, Walter U (1992) Concentration and regulation of cyclic nucleotides, cyclic-nucleotide-dependent protein kinases and one of their major substrates in human platelets. Estimating the rate of cAMP-regulated and cGMP-regulated protein phosphorylation in intact cells. Eur J Biochem 205:471–481.

Flynn KC (2013) The cytoskeleton and neurite initiation. Bioarchitecture 3:86–109.

Gertler FB, Comer AR, Juang JL, Ahern SM, Clark MJ, Liebl EC, Hoffmann FM (1995) enabled, a dosage-sensitive suppressor of mutations in the Drosophila Abl tyrosine kinase, encodes an Abl substrate with SH3 domain-binding properties. Genes Dev 9:521–533.

Gertler FB, Doctor JS, Hoffmann FM (1990) Genetic suppression of mutations in the Drosophila abl proto-oncogene homolog. Science 248:857–860.

Gertler FB, Niebuhr K, Reinhard M, Wehland J, Soriano P (1996) Mena, a relative of VASP and Drosophila Enabled, is implicated in the control of microfilament dynamics. Cell 87:227–239.

Gilman SR, Chang J, Xu B, Bawa TS, Gogos JA, Karayiorgou M, Vitkup D (2012) Diverse types of genetic variation converge on functional gene networks involved in schizophrenia. Nat Neurosci 15:1723–1728.

Goh CS, Bogan AA, Joachimiak M, Walther D, Cohen FE (2000) Co-evolution of proteins with their interaction partners. J Mol Biol 299:283–293.

Goodman CS (1984) Landmarks and Labels That Help Developing Neurons Find Their Way. Bioscience 34:300–307.

Harbeck B, Hüttelmaier S, Schluter K, Jockusch BM, Illenberger S (2000) Phosphorylation of the vasodilator-stimulated phosphoprotein regulates its interaction with actin. J Biol Chem 275:30817–30825.

Hedgecock EM, Culotti JG, Hall DH (1990) The unc-5, unc-6, and unc-40 genes guide circumferential migrations of pioneer axons and mesodermal cells on the epidermis in C. elegans. Neuron 4:61–85.

Hedges SB, Marin J, Suleski M, Paymer M, Kumar S (2015) Tree of life reveals clock-like speciation and diversification. Mol Biol Evol 32:835–845.

Howe AK, Hogan BP, Juliano RL (2002) Regulation of Vasodilator-stimulated Phosphoprotein Phosphorylation and Interaction with Abl by Protein Kinase A and Cell

Adhesion *. J Biol Chem 277:38121–38126.

Hoyng SA, de Winter F, Tannemaat MR, Blits B, Malessy MJA, Verhaagen J (2015) Gene therapy and peripheral nerve repair: a perspective. Front Mol Neurosci 8:32.

Iñiguez LP, Hernández G (2017) The Evolutionary Relationship between Alternative Splicing and Gene Duplication. Front Genet 8:14.

Keenan S, Wetherill SJ, Ugbode CI, Chawla S, Brackenbury WJ, Evans GJO (2017) Inhibition of N1-Src kinase by a specific SH3 peptide ligand reveals a role for N1-Src in neurite elongation by L1-CAM. Sci Rep 7:43106.

Kolodkin AL, Matthes DJ, O'Connor TP, Patel NH, Admon A, Bentley D, Goodman CS (1992) Fasciclin IV: sequence, expression, and function during growth cone guidance in the grasshopper embryo. Neuron 9:831–845.

Kolodkin AL, Pasterkamp RJ (2013) SnapShot: Axon guidance II. Cell 153:722.e1.

Krause M, Dent EW, Bear JE, Loureiro JJ, Gertler FB (2003) Ena/VASP proteins: regulators of the actin cytoskeleton and cell migration. Annu Rev Cell Dev Biol 19:541–564.

Kwiatkowski AV, Gertler FB, Loureiro JJ (2003) Function and regulation of Ena/VASP proteins. Trends Cell Biol 13:386–392.

Lambrechts A, Kwiatkowski AV, Lanier LM, Bear JE, Vandekerckhove J, Ampe C, Gertler FB (2000) cAMP-dependent protein kinase phosphorylation of EVL, a Mena/VASP relative, regulates its interaction with actin and SH3 domains. J Biol Chem 275:36143–36151.

Lanier LM, Gates MA, Witke W, Menzies AS, Wehman AM, Macklis JD, Kwiatkowski D, Soriano P, Gertler FB (1999) Mena is required for neurulation and commissure formation. Neuron 22:313–325.

Lebrand C, Dent EW, Strasser GA, Lanier LM, Krause M, Svitkina TM, Borisy GG, Gertler FB (2004) Critical role of Ena/VASP proteins for filopodia formation in neurons and in function downstream of netrin-1. Neuron 42:37–49.

Levi-Montalcini R, Hamburger V (1953) A diffusible agent of mouse sarcoma, producing hyperplasia of sympathetic ganglia and hyperneurotization of viscera in the chick embryo. J Exp Zool 123:233–287.

Lewis PA, Bradley IC, Pizzey AR, Isaacs HV, Evans GJO (2017) N1-Src Kinase Is Required for Primary Neurogenesis in Xenopus tropicalis. J Neurosci 37:8477–8485.

Liu G, Beggs H, Jürgensen C, Park H-T, Tang H, Gorski J, Jones KR, Reichardt LF, Wu J, Rao Y (2004) Netrin requires focal adhesion kinase and Src family kinases for axon outgrowth and attraction. Nat Neurosci 7:1222–1232.

Loureiro JJ, Rubinson DA, Bear JE, Baltus GA, Kwiatkowski AV, Gertler FB (2002) Critical roles of phosphorylation and actin binding motifs, but not the central proline-rich region, for Ena/vasodilator-stimulated phosphoprotein (VASP) function during cell migration. Mol Biol Cell 13:2533–2546.

Maden M (2007) Retinoic acid in the development, regeneration and maintenance of the nervous system. Nat Rev Neurosci 8:755–765.

Maness PF (1992) Nonreceptor protein tyrosine kinases associated with neuronal development. Dev Neurosci 14:257–270.

Maness PF, Aubry M, Shores CG, Frame L, Pfenninger KH (1988) c-src gene product in developing rat brain is enriched in nerve growth cone membranes. Proc Natl Acad Sci U S A 85:5001–5005.

Martinez R, Mathey-Prevot B, Bernards A, Baltimore D (1987) Neuronal pp60c-src contains a six-amino acid insertion relative to its non-neuronal counterpart. Science 237:411–415.

Mira H, Morante J (2020) Neurogenesis From Embryo to Adult - Lessons From Flies and Mice. Front Cell Dev Biol 8:533.

Ngoka LCM (2008) Sample prep for proteomics of breast cancer: proteomics and gene ontology reveal dramatic differences in protein solubilization preferences of radioimmunoprecipitation assay and urea lysis buffers. Proteome Sci 6:30.

Pasterkamp RJ, Kolodkin AL (2013) SnapShot: Axon Guidance. Cell 153:494, 494e1–e2.

Pistor S, Chakraborty T, Niebuhr K, Domann E, Wehland J (1994) The ActA protein of Listeria monocytogenes acts as a nucleator inducing reorganization of the actin cytoskeleton. EMBO J 13:758–763.

Rottner K, Behrendt B, Small JV, Wehland J (1999) VASP dynamics during lamellipodia protrusion. Nat Cell Biol 1:321–322.

Ryan JF, Chiodin M (2015) Where is my mind? How sponges and placozoans may have lost neural cell. Available at: http://dx.doi.org/10.1098/rstb.2015.0059.

Schwede F, Christensen A, Liauw S, Hippe T, Kopperud R, Jastorff B, Døskeland SO (2000) 8-Substituted cAMP analogues reveal marked differences in adaptability, hydrogen bonding, and charge accommodation between homologous binding sites (AI/AII and BI/BII) in cAMP kinase I and II. Biochemistry 39:8803–8812.

Seeger M, Tear G, Ferres-Marco D, Goodman CS (1993) Mutations affecting growth cone guidance in Drosophila: genes necessary for guidance toward or away from the midline. Neuron 10:409–426.

Serafini T, Kennedy TE, Gaiko MJ, Mirzayan C, Jessell TM, Tessier-Lavigne M (1994) The netrins define a family of axon outgrowth-promoting proteins homologous to C. elegans UNC-6. Cell 78:409–424.

Sierra-Fonseca JA, Najera O, Martinez-Jurado J, Walker EM, Varela-Ramirez A, Khan AM, Miranda M, Lamango NS, Roychowdhury S (2014) Nerve growth factor induces neurite outgrowth of PC12 cells by promoting Gβγ-microtubule interaction. BMC Neurosci 15:1–19.

Sperry RW (1943) Effect of 180 degree rotation of the retinal field on visuomotor coordination. J Exp Zool 92:263–279.

Sperry RW (1963) CHEMOAFFINITY IN THE ORDERLY GROWTH OF NERVE FIBER PATTERNS AND CONNECTIONS. Proc Natl Acad Sci U S A 50:703–710.

Stehelin D, Varmus HE, Bishop JM, Vogt PK (1976) DNA related to the transforming gene(s) of avian sarcoma viruses is present in normal avian DNA. Nature 260:170–173.

Stoeckli ET (2018) Understanding axon guidance: are we nearly there yet? Development 145 Available at: http://dx.doi.org/10.1242/dev.151415.

Tani K, Sato S, Sukezane T, Kojima H, Hirose H, Hanafusa H, Shishido T (2003) Abl interactor 1 promotes tyrosine 296 phosphorylation of mammalian enabled (Mena) by c-Abl kinase. J Biol Chem 278:21685–21692.

Weiss P (1941) Further Experiments with Deplanted and Deranged Nerve Centers in Amphibians. Proc Soc Exp Biol Med 46:14–15.

Wills Z, Bateman J, Korey CA, Comer A, Van Vactor D (1999) The tyrosine kinase Abl and its substrate enabled collaborate with the receptor phosphatase Dlar to control motor axon guidance. Neuron 22:301–312.

https://www.biodiversitylibrary.org/item/103261#page/685/mode/1up

S. Ramon y Cajal (1909) Histologie du Systeme Nerveux de i'Homme et des Vertebres (Consejo Superior de Investigaciones Cientificas 1909).

Appendix
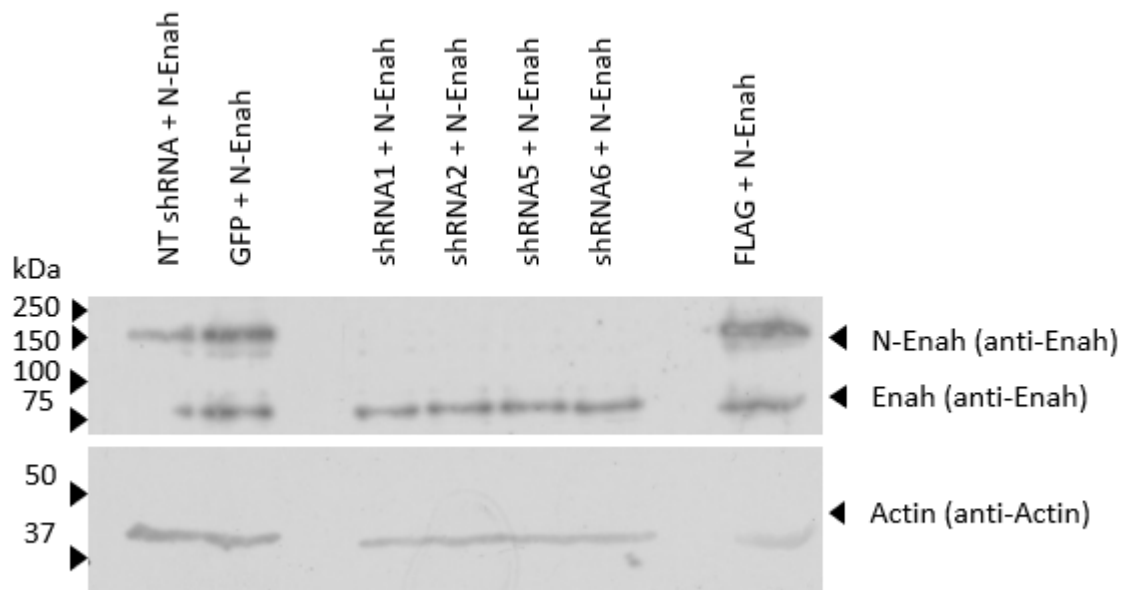
Figure 14. N-Enah is effectively knocked down by shRNAs designed to target the neural exon. N-Enah-WT was co-transfected into B104 cells with non-targeting control shRNA (NT), pSUPER-GFP-shRNA1, pSUPER-GFP-shRNA2, pSUPER-CFP-shRNA5 or pSUPER-CFP-shRNA6. The targeting sequences of shRNA1 and shRNA5 are the same except that shRNA1 is in a plasmid expressing the GFP reporter gene and shRNA5 is in a plasmid expressing the CFP reporter gene. The targeting sequences of shRNA3 and shRNA6 are the same except that shRNA2 is in a plasmid expressing the GFP reporter gene and shRNA6 is in a plasmid expressing the CFP reporter gene. The cells were lysed 2.5 days after transfection and then analysed by Western blotting with Enah or actin antibodies. Lanes 1 and 2 are negative controls that control for the targeting sequences of the shRNAs and the pSUPER plasmid backbone, respectively. The last lane is a positive control for N-Enah.